Inorganic Chemistry

Article

pubs.acs.org/IC

Assembly of Organic–Inorganic Hybrid Supramolecular Materials Based on Basketlike {M⊂$P_6Mo_{18}O_{73}$} (M = Ca, Sr, Ba) Cage and Transition-Metal Complex

Kai Yu,[†,‡] Bin Wan,[†,‡] Yang Yu,[†,‡] Lu Wang,[§] Zhan-hua Su,[†,‡] Chun-mei Wang,[†,‡] Chun-xiao Wang,[†,‡] and Bai-Bin Zhou*[,†,‡]

[†]Key Laboratory for Photonic and Electronic Bandgap Materials, Ministry of Education, School of Chemistry and Chemical Engineering, Harbin Normal University, Harbin 150025, People's Republic of China

[‡]Key Laboratory of Synthesis of Functional Materials and Green Catalysis, Colleges of Heilongjiang Province, Harbin Normal University, Harbin, 150025, People's Republic of China

[§]Department of Biochemical Engineering, Harbin Institute of Technology, Harbin, Heilongjiang 150090, People's Republic of China

Supporting Information

ABSTRACT: Eight members of basketlike mixed-valent compounds, formulated as $\{H_3O\}_2\{Fe^{III}(2,2'\text{-bpy})_3\}_6\{Sr\subset P_6Mo^{V}_4Mo^{VI}_{14}O_{73}\}_2\cdot 9H_2O$ (**1**), $\{H_2(4,4'\text{-bpy})\}_5\{[Ni(4,4'\text{-bpy})(H_2O)_3]_2[Ni(H_2O)_2][Sr\subset P_6Mo^{V}_2Mo^{VI}_{16}O_{73}]_2\}\cdot 12H_2O$ (**2**), $\{Cu_2(bim)_4(H_2O)\}_2\{[Cu(bim)_2]_2[Cu(bim)(H_2O)]_2Cu(H_2O)_2\text{-}[Sr\subset P_6Mo^{V}_3Mo^{VI}_{15}O_{73}]_2\}\cdot 16H_2O$ (**3**), $\{H_3O\}_4\{[Cd(phen)_2]_2Sr(H_2O)_5\text{-}[Sr\subset P_6Mo^{V}_4Mo^{VI}_{14}O_{73}]\}\cdot H_2O$ (**4**), $\{Cu(bim)_2\}\{[Cu(bim)_2]_2[Cu(Hbim)(H_2O)_2]\text{-}[Ca\subset P_6Mo^{V}_3Mo^{VI}_{15}O_{73}]\}\cdot 9H_2O$ (**5**), $\{[Cu(2,2'\text{-bpy})(H_2O)]_4\text{-}[Ca\subset P_6Mo^{V}_2Mo^{VI}_{16}O_{73}]\}\cdot 4H_2O$ (**6**), $\{[Cu(2,2'\text{-bpy})(H_2O)]_4[Sr\subset P_6Mo^{V}_2Mo^{VI}_{16}O_{73}]\}\cdot 8H_2O$ (**7**), and $\{[Cu(2,2'\text{-bpy})(H_2O)]_4\text{-}[Ba\subset P_6Mo^{V}_2Mo^{VI}_{16}O_{73}]\}\cdot 8H_2O$ (**8**), have been hydrothermally synthesized and structurally characterized via elemental analysis, thermogravimetry (TG), infrared (IR) spectroscopy, ultraviolet–visible light (UV-vis) spectroscopy, X-ray photoelectron spectroscopy (XPS), and single-crystal X-ray diffraction (XRD). The structural analysis shows that all the compounds contain basket-shaped polyoxoanions $[M\subset P_6Mo^{V}_nMo^{VI}_{18-n}O_{73}]^{(6+n)-}$ (M = Ca, Sr, Ba; n = 2, 3, or 4) (abbreviated as $\{P_6Mo_{18}O_{73}\}$) as building units, which consists of a tetravacant γ-Dawson-type$\{P_2Mo_{14}\}$ unit and a "handle"-shaped $\{P_4Mo_4\}$ segment encapsulating a single alkaline-earth metals cation M^{2+} in the central cavity. Compound **1** presents a zero-supported basketlike structure decorated by three discrete $\{Fe(2,2'\text{-bipy})_3\}$ fragments. Compound **2** is monosupported by $\{Ni(4,4'\text{-bipy})(H_2O)_3\}$ subunit. Compound **3** and **4** are bisupported by copper complexes and cadmium complexes, respectively. Compound **5** exhibit a trisupported basket cluster modified with two $\{Cu(bim)_2\}^{2+}$ and one $\{Cu(Hbim)(H_2O)\}^{3+}$ cations. Compounds **6**–**8** are isostructural clusters exhibiting similar tetra-supported structures. Compound **1**, **2**, and **4** represent the first basket-like hybrids containing transition-metal iron, nickel, and cadmium, respectively. In addition, compounds **2**, **6**, **7**, and **8** are observed for the first time as a two-electron-reduced basket form. The compounds display good electrocatalytic activity upon the reduction of nitrite, and fluorescent properties.

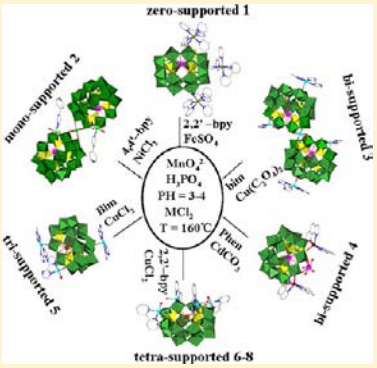

INTRODUCTION

Organic–inorganic hybrid materials have received great research attention in creating nanoscale structures and supramolecular assemblies, because of their extensive theoretical and practical applications in catalysis,[1a] gas storage and adsorption,[1b−d] electromagnetic functional materials,[1e−g] biomedicine,[1h] and photochemistry.[1i,j] Nowadays, the development of materials chemistry is mostly dependent on the synthesis of compounds holding new structures and properties. One promising approach for the design of organic–inorganic hybrid materials is to build connections between the surface oxygen atoms of POMs and various organic units or transition-metal complex moieties.[2,3] Organic components can dramatically influence microstructure of hybrid materials. In addition, the synergic interactions between organic and inorganic components may be exploited in the preparation of hybrid materials exhibiting composite properties or even new characters. Thus, the selection of suitable metal, organic ligands, and inorganic building units is the main factor for the design and construction of organic–inorganic hybrids. The transition-metal ions have been widely used as the linking units to construct the hybrid compounds, because of their relatively strong coordination abilities with both terminal O atoms of POM and N atoms of organic ligand. On the other hand, the rigid organic ligands with N-donors (such as imidazole, 4,4′-bipyridine, 2,2′-biimidazole, and 1,10-phenanthroline, etc.) not only may be introduced into a hybrid system to coordinate with

Received: October 31, 2012
Published: December 18, 2012

secondary metal but also may provide recognition sites for $\pi-\pi$ stacking interactions to form interesting supramolecular structures. Thus, these ligands have been extensively employed as organic template reagents for the fabrication of infinite one-dimensional (1D), two-dimensional (2D), and even three-dimensional (3D) supramolecular arrays through weak intermolecular interactions,[4] including hydrogen bonding, $\pi-\pi$ stacking, weak van der Waals forces, etc.

As a unique class of metalloxide clusters, heteropoly blues with deep blue color, have recently been employed as inorganic building units for constructing supramolecular hybrid arrays with various organic ligands or metal−organic coordination fragments.[5−10] The kinds of mixed-valence molybdates or tungstates are obtained by one (or more)-electron reduction of the corresponding Mo^{VI} and W^{VI} polyoxoanions. The added electrons could be either localized on a metal center or delocalized as "extra" electrons over several metal centers. As a result, the electron density and activity of the surface oxygen atoms of POM were effectively modified, which can induce more cationic linking units into the crystal structures and lead to plenty of structural topologies. On the other hand, heteropoly blues can release a defined number of their blue electrons at appropriate redox ambiance, so they are potential reducing agents and exhibit interesting mixed-valence electron delocalization or electrochemical properties that are related to the electron-transfer reactions within the clusters.[6] In addition, the redox-active nature of molybdenum or tungsten in such POM could provide potentially new types of catalyst and magnetic systems.[7,8e]

To date, many organic−inorganic hybrids based on heteropoly blues building blocks have been synthesized and studied. However, it is worth noting that most of these studies focus on classical heteropolyanions, such as the Keggin-type,[7] the Wells−Dawson heteropoly blues,[8] and their derivatives. Compared with classical heteropoly blues, the unclassical mixed-valence compounds have been far unexplored for their lability in solution.[9,10] In particular, the basket-like $\{P_6Mo_{18}O_{73}\}$ cages are still less common. Since the first example of a basketlike compound, $[H_2dmpip]_5[K\subset P_6Mo_{18}O_{73}]$ was reported by the Zhang group,[10a] two 0D hybrids based on basketlike POMs and transition-metal complexes $[Cu(phen)(H_2O)_3][\{Cu(phen)(H_2O)_2\}\{Cu(phen)(H_2O)\}_3\{Sr\subset P_6Mo_{18}O_{73}\}]\cdot 3H_2O$[10b] and $[Cu_4(bpy)_4(H_2O)_4K\subset P_6Mo_{18}O_{73}]\cdot 7H_2O$[10c] have been reported. More recently, the first 1D example, $(H_2imi)_6(Himi)_4\{[Sr(H_2O)_4]_2[Sr\subset P_6Mo_{18}O_{73}]_2\}\cdot 17H_2O$,[10d] was reported by our group. Hitherto, only the above four $\{P_6Mo_{18}O_{73}\}$-based compounds have been reported. Therefore, further research is necessary to enrich and develop this branch. In our continuing research on hybric supramolecular assemblies, we choose the basketlike $\{P_6Mo_{18}O_{73}\}$-based hybrid system as our research project. The reasons are triple: (a) The mixed-valence Mo centers lead to the high negative charges of the entire clusters, which can induce more transition-metal complex units into the crystal structures; (b) In addition, calculations of geometry and studies of the density functional theory (DFT) show that the basket-shaped $\{P_6Mo_{18}O_{73}\}$ heteropolyanion is a possible ligand to coordinate metal ions via external terminal P−O and molybdate oxygen sites at the "handle" of the basket.[10c] (c) Because of the larger steric hindrance of basketlike POMs, they are valuable building blocks for tailor-made inorganic and organic or organic hybrid materials by hydrogen bonding and $\pi-\pi$ stacking interactions. Thus, we are interested in employing metal−organic units to decorate these high-nuclear clusters in order to get new hybrid materials to explore their fascinating electrochemical and electrocatalytic properties. Furthermore, the alkali-metal (K^+, Na^+) ions usually act as a template to be trapped by the cagelike and cryptate compounds, because of their flexible coordination modes and relatively high concentration in the starting materials.[10a,c,11] In contrast, cagelike or cryptate POMs encapsulating alkaline-earth metal ions remain far less developed, and only a few examples have been reported so far.[12] In fact, alkaline-earth metal ions (Ca^{2+}, Sr^{2+}, and Ba^{2+}) not only contain the charge number of transition-metal ions, but also possess the coordination mode and size of lanthanide ions. So they might be good template candidates for cryptand hybrids to fill in cavum of POM to stabilize the entire cryptand POM.

Based on previous work,[10b,d] we attempt to change the ligand and metal centers of TMCs and introduce Ca^{2+} and Ba^{2+} into the basketlike POMs system to act as templates, following previous K^+ and Sr^{2+}, which lead to a series of basketlike compounds, namely, $\{H_3O\}_2\{Fe^{III}(2,2'\text{-bpy})_3\}_6\{Sr\subset P_6Mo^{V}_4Mo^{VI}_{14}O_{73}\}_2\cdot 9H_2O$ (**1**), $\{H_2(4,4'\text{-bpy})\}_5\{[Ni(4,4'\text{-bpy})(H_2O)_3]_2[Ni(H_2O)_2]\text{-}[Sr\subset P_6Mo^{V}_2Mo^{VI}_{16}O_{73}]_2\}\cdot 12H_2O$ (**2**), $\{Cu_2(bim)_4(H_2O)\}_2\{[Cu(bim)_2]_2[Cu(bim)(H_2O)]_2Cu\text{-}(H_2O)_2[Sr\subset P_6Mo^{V}_3Mo^{VI}_{15}O_{73}]_2\}\cdot 16H_2O$ (**3**), $\{H_3O\}_4\{[Cd\text{-}(phen)_2]_2Sr(H_2O)_5[Sr\subset P_6Mo^{V}_4Mo^{VI}_{14}O_{73}]\}\cdot H_2O$ (**4**), $\{Cu\text{-}(bim)_2\}\{[Cu(bim)_2]_2[Cu(Hbim)(H_2O)_2]\text{-}[Ca\subset P_6Mo^{V}_3Mo^{VI}_{15}O_{73}]\}\cdot 9H_2O$ (**5**), $\{[Cu(2,2'\text{-}bpy)(H_2O)]_4[Ca\subset P_6Mo^{V}_2Mo^{VI}_{16}O_{73}]\}\cdot 4H_2O$ (**6**), $\{[Cu(2,2'\text{-}bpy)(H_2O)]_4[Sr\subset P_6Mo^{V}_2Mo^{VI}_{16}O_{73}]\}\cdot 8H_2O$ (**7**), and $\{[Cu\text{-}(2,2'\text{-bpy})(H_2O)]_4[Ba\subset P_6Mo^{V}_2Mo^{VI}_{16}O_{73}]\}\cdot 8H_2O$ (**8**), which have different degrees of reduction, and their electrocatalytic and fluorescence properties were also investigated.

EXPERIMENTAL SECTION

General Methods and Materials. All chemicals were commercially purchased and used without further purification. Elemental analyses (C, H, and N) were performed on a Perkin−Elmer Model 2400 CHN elemental analyzer; P, Mo, Ni, Cu, Cd, Fe, Ca, Sr, and Ba were analyzed on a PLASMA-SPEC (I) ICP atomic emission spectrometer. IR spectrum was recorded in the range 400−4000 cm^{-1} on an Alpha Centaurt FT/IR Spectrophotometer using KBr pellets. Diffuse-reflectance UV−vis spectra ($BaSO_4$ pellets) were obtained with a Varian Cary 500 UV−vis NIR spectrometer. X-ray photoelectron spectroscopy (XPS) analyses were performed on a VG ESCALAB MK II spectrometer with a Mg Kα (1253.6 eV) achromatic X-ray source. Thermogravimetry (TG) analyses were performed on a Perkin−Elmer Model TGA7 instrument in flowing N_2 with a heating rate of 10 °C min^{-1}. The electrochemical measurement was carried out on a CHI Model 660 electrochemical workstation at room temperature (25−30 °C). A conventional three-electrode system was used. The working electrode was a carbon paste electrode (CPE), with a Pt wire as the counter electrode, and a Ag/AgCl (3 M KCl) electrode was used as a reference electrode. Fluorescence spectra were performed on a Hitachi Model F-4500 fluorescence/phosphorescence spectrophotometer with a 450-W xenon lamp as the excitation source.

Synthesis of $\{H_3O\}_2\{Fe^{III}(2,2'\text{-bipy})_3\}_6\text{-}\{Sr\subset P_6Mo^{V}_4Mo^{VI}_{14}O_{73}\}_2\cdot 9H_2O$ (1). A mixture of $Na_2MoO_4\cdot 2H_2O$ (1.210 g, 5.00 mmol), $FeSO_4\cdot 7H_2O$ (0.417 g, 1.50 mmol), 2,2′-bpy (0.434 g, 2.78 mmol), H_3PO_4 (1 mL, 15 mmol), $SrCl_2\cdot 6H_2O$ (0.667 g, 2.50 mmol), and H_2O (27 mL, 1.5 mol) was stirred at room temperature for 30 min; the pH value then was adjusted to ∼3.5 with 1 M NaOH, and it was sealed in a 50-mL Teflon-lined stainless steel reactor, which was heated at 160 °C for 4 days. The dark-blue crystals were isolated and collected by filtration, washed thoroughly with

dx.doi.org/10.1021/ic302311q | Inorg. Chem. 2013, 52, 485−498

Table 1. X-ray Crystallographic Data for Compounds 1−8

	1	2	3	4
formula	$C_{180}H_{168}N_{36}O_{157}P_{12}Fe_6Mo_{36}Sr_2$	$C_{70}H_{106}N_{14}O_{166}P_{12}Ni_3Mo_{36}Sr_2$	$C_{84}H_{130}N_{56}O_{168}P_{12}Cu_9Mo_{36}Sr_2$	$C_{48}H_{52}N_8O_{81}P_6Cd_2Mo_{18}Sr_2$
Fw (g mol^{-1})	9683.32	7976.34	9185.03	4349.75
crystal system	triclinic	triclinic	triclinic	orthorhombic
space group	$P\bar{1}$	$P\bar{1}$	$P\bar{1}$	$Cmc2(1)$
a (Å)	16.9005(8)	25.826(6)	14.8731(5)	28.9375(7)
b (Å)	19.1214(9)	13.748(3)	16.1687(5)	20.1919(5)
c (Å)	22.7492(11)	28.348(7)	25.5045(8)	20.3956(5)
α (deg)	86.1230(10)	90	96.4870(10)	90
β (deg)	86.4480(10)	99.835(4)	101.8410(10)	90
γ (deg)	79.0750(10)	90.00	103.4290(10)	90
V (Å)	7192.8(6)	9917(4)	5754.9(3)	11917.2(5)
Z	1	2	1	4
d_{calcd} (Mg cm^{-3})	2.235	2.670	2.647	2.422
μ (mm^{-1})	2.339	3.218	3.363	3.242
GOF on F^2	1.026	1.021	1.028	1.048
final R indices $[I > 2\sigma(I)]$				
$R_1{}^a$	0.0386	0.0351	0.0316	0.0634
$wR_2{}^b$	0.1022	0.0754	0.0841	0.1668
	5	**6**	**7**	**8**
formula	$C_{42}H_{64}N_{28}O_{84}P_6Cu_4Mo_{18}Ca$	$C_{40}H_{48}CaCu_4Mo_{18}N_8O_{81}P_6$	$C_{40}H_{56}Cu_4Mo_{18}N_8O_{85}P_6Sr$	$C_{40}H_{56}BaCu_4Mo_{18}N_8O_{85}P_6$
Fw (g mol^{-1})	4512.23	4143.89	4263.49	4313.20
crystal system	triclinic	monoclinic	monoclinic	monoclinic
space group	$P\bar{1}$	$C2/c$	$C2/c$	$C2/c$
a (Å)	16.4721(4)	17.9532(6)	17.925(5)	17.9957(5)
b (Å)	17.2850(4)	27.2820(9)	27.308(7)	27.2288(7)
c (Å)	20.1103(4)	23.9355(8)	23.877(9)	23.9077(6)
α (deg)	97.29	90	90	90
β (deg)	91.17	99.9810(10)	99.829(3)	99.47
γ (deg)	95.90	90	90	90
V (Å)	5646.2(2)	11546.2(7)	7192.8(6)	11555.0(5)
Z	2	4	4	4
d_{calcd} (Mg cm^{-3})	2.655	2.384	2.459	2.479
μ (mm^{-1})	2.914	2.832	3.258	3.124
GOF on F^2	1.039	1.054	1.040	1.060
final R indices $[I > 2\sigma(I)]$				
$R_1{}^a$	0.0244	0.0490	0.0450	0.0401
$wR_2{}^b$	0.0698	0.1668	0.1544	0.1594

$^aR_1 = \sum||F_o| - |F_c||/\sum|F_o|$. $^bwR_2 = \{Rw[(|F_o)^2 - (|F_c)^2]^2/Rw[(|F_o)^2]^2\}^{1/2}$.

distilled water, and dried at room temperature (yield: 40%, based on Mo). Anal. Calcd. for $C_{180}H_{168}N_{36}O_{157}P_{12}Fe_6Mo_{36}Sr_2$ (M_r = 9683.32): C, 22.32; H, 1.75; N, 5.21; P, 3.84; Fe, 3.46; Mo, 35.67; Sr, 1.81. Found: C, 22.28; H, 1.79; N, 5.16; P, 3.90; Fe, 3.42; Mo, 35.70; Sr, 1.85. IR (KBr pellet, cm^{-1}): 3428 (br), 3270 (br), 3014 (m), 1628 (s), 1147 (s), 1031 (m), 965 (s), 741 (s), 691 (s), 617 (s), 509 (s).

Synthesis of $\{H_2(4,4'\text{-bipy})\}_5\{[Ni(4,4'\text{-bipy})(H_2O)_3]_2[Ni(H_2O)_2][SrP_6Mo^V_2Mo^{VI}_{16}O_{73}]_2\}\cdot 12H_2O$ (2). A mixture of $Na_2MoO_4\cdot 2H_2O$ (1.210 g, 5.00 mmol), $NiCl_2\cdot 6H_2O$ (0.357 g, 1.5 mmol), 4,4′-bpy (0.434 g, 2.78 mmol), H_3PO_4(1 mL, 15 mmol), $SrCl_2\cdot 6H_2O$ (0.667 g, 2.50 mmol), and H_2O (27 mL, 1.5 mol) was stirred at room temperature for 30 min; the pH value then was adjusted to ∼3.5 with 1 M NaOH, and it was sealed in a 50-mL Teflon-lined stainless steel reactor, which was heated at160 °C for 4 days. The dark-blue crystals were isolated and collected by filtration, washed thoroughly with distilled water, and dried at room temperature (yield: 56%, based on Mo). Anal. Calcd. for $C_{70}H_{106}N_{14}O_{166}P_{12}Ni_3Mo_{36}Sr_2$ (M_r = 7976.34): C, 10.54; H, 1.34; N, 2.46; P, 4.66; Ni, 2.21; Mo, 43.30; Sr, 2.20. Found: C, 10.50; H, 1.40; N, 2.41; P, 4.71; Ni, 2.17; Mo, 43.35; Sr, 2.18. IR (KBr pellet, cm^{-1}): 3420 (br), 3262 (br), 3112 (m), 1645 (s), 1504 (m), 1132 (s), 964 (s), 740 (s), 674 (s), 617 (s), 509 (w).

Synthesis of $\{Cu_2(bim)_4(H_2O)\}_2\{[Cu(bim)_2]_2[Cu(bim)(H_2O)]_2Cu(H_2O)_2[SrP_6Mo^V_3Mo^{VI}_{15}O_{73}]_2\}\cdot 16H_2O$ (3). A mixture of $Na_2MoO_4\cdot 2H_2O$ (1.210 g, 5.00 mmol), $CuC_2O_4\cdot{}^1/_2H_2O$ (0.241g, 1.5 mmol), bim (0.373 g, 2.78 mmol), H_3PO_4 (1 mL, 15 mmol), $SrCl_2\cdot 6H_2O$ (0.667 g, 2.50 mmol), and H_2O (27 mL, 1.5 mol) was stirred at room temperature for 30 min; the pH value then was adjusted to ∼3.5 with 1 M NaOH, and it was sealed in a 50-mL Teflon-lined stainless steel reactor, which was heated at 160 °C for 4 days. The dark-blue crystals were isolated and collected by filtration, washed thoroughly with distilled water, and dried at room temperature (yield: 47%, based on Mo). Anal. Calcd. for $C_{84}H_{130}N_{56}O_{168}P_{12}Cu_9Mo_{36}Sr_2$ (M_r = 9185.03): C, 10.98; H, 1.43; N, 8.54; P, 4.05; Cu, 6.23; Mo, 37.60; Sr, 1.91. Found: C, 10.92; H, 1.48; N, 8.51; P, 3.99; Cu, 6.29; Mo, 37.66; Sr, 1.87. IR (KBr pellet, cm^{-1}): 3417 (br), 3125 (sh), 3010 (br), 1637 (s), 1507 (s), 1180 (s), 978 (s), 764 (s), 641 (s), 618 (s), 512 (s).

Synthesis of $\{H_3O\}_4\{[Cd(phen)_2]_2Sr(H_2O)_5[SrP_6Mo^V_4Mo^{VI}_{14}O_{73}]\}\cdot H_2O$ (4). A mixture of $Na_2MoO_4\cdot 2H_2O$ (1.210 g, 5.00 mmol), $CdCO_3$ (0.259 g, 1.5 mmol), phen (0.501 g, 2.78 mmol), H_3PO_4 (1 mL, 15 mmol), and $SrCl_2\cdot 6H_2O$ (0.667 g, 2.50 mmol), and H_2O (27 mL, 1.5 mol) was stirred at room temperature for 30 min; the pH value then was adjusted to ∼3.5 with 1 M NaOH, and it was sealed in a 50-mL Teflon-lined stainless steel reactor, which was heated at 160 °C for 4 days. The dark-blue crystals were isolated and collected by filtration, washed thoroughly with distilled water, and

dx.doi.org/10.1021/ic302311q | Inorg. Chem. 2013, 52, 485−498

Scheme 1. Illustration of the Relationship between Basket-Type Crystalline Products and Different Template Reagents

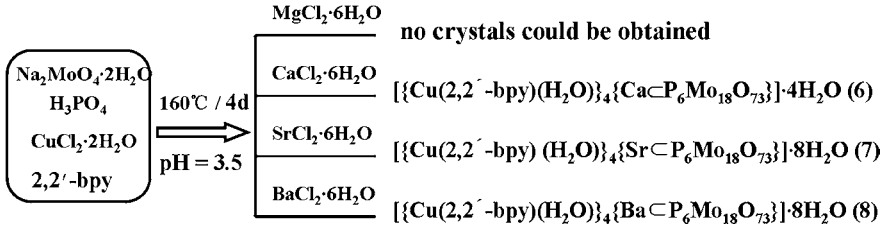

dried at room temperature (yield: 45%, based on Mo). Anal. Calcd. for $C_{48}H_{56}N_8O_{83}P_6Cd_2Mo_{18}Sr_2$ (M_r = 4385.84): C, 13.14; H, 1.29; N, 2.56; P, 4.24; Cd, 5.13; Mo, 39.37; Sr, 4.00. Found: C, 13.19; H, 1.34; N, 2.51; P, 4.18; Cd, 5.07; Mo, 39.42; Sr, 4.02. IR (KBr pellet, cm^{-1}): 3427 (br), 3403 (w), 3055 (w), 1628 (s), 1512 (s), 1421 (s), 1073 (s), 932 (s), 849 (s), 775 (s), 691 (m), 592 (m).

Synthesis of $[Cu(bim)_2]\{[Cu(bim)_2]_2Cu(Hbim)(H_2O)_2[Ca⊂P_6Mo^V_3Mo^{VI}_{15}O_{73}]\}\cdot 9H_2O$ (5). A mixture of $Na_2MoO_4\cdot 2H_2O$ (1.210 g, 5.00 mmol), $CuCl_2\cdot 2H_2O$ (0.256 g, 1.50 mmol), bim (0.373 g, 2.78 mmol), H_3PO_4 (1 mL, 15 mmol), $CaCl_2\cdot 2H_2O$ (0.368 g, 2.50 mmol), and H_2O (27 mL, 1.5 mol) was stirred at room temperature for 30 min; the pH value then was adjusted to ~3.5 with 1 M NaOH, and it was sealed in a 50-mL Teflon-lined stainless steel reactor, which was heated at 160 °C for 4 days. The dark-blue crystals were isolated and collected by filtration, washed thoroughly with distilled water, and dried at room temperature (yield: 52%, based on Mo). Anal. Calcd. for $C_{42}H_{64}N_{28}O_{84}P_6Cu_4Mo_{18}Ca$ (M_r = 4512.23): C, 11.18; H, 1.43; N, 8.69; P, 4.12; Cu, 5.63; Mo, 38.27; Ca, 0.89. Found: C, 11.24; H, 1.49; N, 8.63; P, 4.07; Cu, 5.58; Mo, 38.32; Ca, 0.87. IR (KBr pellet, cm^{-1}): 3484 (br), 3167 (s), 3083 (m), 1620 (s), 1446 (m), 1073 (s), 932 (s), 841 (s), 775 (s), 601 (s), 542 (w).

Synthesis of $\{[Cu(2,2'\text{-bpy})(H_2O)]_4[Ca⊂P_6Mo^V_2Mo^{VI}_{16}O_{73}]\}\cdot 4H_2O$ (6). A mixture of $Na_2MoO_4\cdot 2H_2O$ (1.210 g, 5.00 mmol), $CuCl_2\cdot 2H_2O$ (0.256 g, 1.50 mmol), 2,2′-bpy (0.434 g, 2.78 mmol), H_3PO_4(1 mL, 15 mmol), $CaCl_2\cdot 2H_2O$ (0.368 g, 2.50 mmol), and H_2O (27 mL, 1.5 mol) was stirred at room temperature for 30 min; the pH value then was adjusted to ~3.5 with 1 M NaOH, and it was sealed in a 50-mL Teflon-lined stainless steel reactor, which was heated at 160 °C for 4 days. The dark-blue crystals were isolated and collected by filtration, washed thoroughly with distilled water, and dried at room temperature (yield: 46%, based on Mo). Anal. Calcd. for $C_{40}H_{56}N_8O_{81}P_6Cu_4Mo_{18}Ca$ (M_r = 4151.89): C, 11.57; H, 1.36; N, 2.70; P, 4.48; Cu, 6.12; Mo, 41.42; Ca, 0.97. Found: C, 11.59; H, 1.35; N, 2.66; P, 4.52; Cu, 6.08; Mo, 41.47; Ca, 1.01. IR (KBr pellet, cm^{-1}): 3450 (br), 3188 (m), 3125 (m), 1652 (s), 1498 (m), 1122 (s), 989 (s), 824 (s), 765 (s), 642 (s).

Synthesis of $\{[Cu(2,2'\text{-bpy})(H_2O)]_4[Sr⊂P_6Mo^V_2Mo^{VI}_{16}O_{73}]\}\cdot 8H_2O$ (7). Compound 7 was prepared similar to the method of compound **6**, except that the initial chemical $CaCl_2\cdot 2H_2O$ was substituted by $SrCl_2\cdot 6H_2O$ (0.667 g, 2.50 mmol). The dark-blue crystals were isolated and collected by filtration, washed thoroughly with distilled water, and dried at room temperature (yield: 54%, based on Mo). Anal. Calcd. for $C_{40}H_{56}N_8O_{56}P_6Cu_4Mo_{18}Sr$ (M_r = 4263.49): C, 11.27; H, 1.32; N, 2.63; P, 4.36; Cu, 5.96; Mo, 40.51; Sr, 2.06. Found: C, 11.29; H, 1.28; N, 2.67; P, 4.31; Cu, 6.01; Mo, 40.48; Sr, 2.10. IR (KBr pellet, cm^{-1}): 3435 (br), 3176 (m), 3120 (m), 1650 (s), 1496 (m), 1123 (s), 990 (s), 820 (s), 764 (s), 640 (s).

Synthesis of $\{[Cu(2,2'\text{-bpy})(H_2O)]_4[Ba⊂P_6Mo^V_2Mo^{VI}_{16}O_{73}]\}\cdot 8H_2O$ (8). Compound **8** was prepared similar to the method of compound **6**, except that the initial chemical $CaCl_2\cdot 2H_2O$ was substituted by $BaCl_2\cdot 2H_2O$ (0.667 g, 2.50 mmol). The dark-blue crystals were isolated and collected by filtration, washed thoroughly with distilled water, and dried at room temperature (yield: 40%, based on Mo). Anal. Calcd. for $C_{40}H_{56}N_8O_{85}P_6Cu_4Mo_{18}Ba$ (M_r = 4313.20): C, 11.14; H, 1.31; N, 2.60; P, 4.31; Cu, 5.89; Mo, 40.04; Ba, 3.18. Found: C, 11.18; H, 1.26; N, 2.65; P, 4.27; Cu, 5.93; Mo, 40.01; Sr, 3.20. IR (KBr pellet, cm^{-1}): 3304 (br), 3179 (m), 3123 (m), 1654 (s), 1494 (m), 1125 (s), 987 (s), 819 (s), 763 (s), 639 (s).

X-ray Crystallography. Single crystal was mounted on a glass fiber, and the data were collected at 293 K on a Bruker SMART CCD diffractometer with graphite-monochromated Mo Kα radiation (λ = 0.71073 Å). Semiempirical absorption correction based on symmetry equivalent reflections was applied. The structure was solved by direct methods and refined by the full-matrix least-squares method based on F^2. Structure solution, refinement, and generation of publication materials were performed with the use of the SHELXTL crystallographic software package.[13] All of the non-hydrogen atoms were refined anisotropically. Hydrogen atoms on carbon atoms of organic ligands were included at calculated positions and refined with a riding model. The H atoms on water molecules were not included and just put into the final molecular formula. A summary of crystal data and structure refinement for compound **1**–**8** is provided in Table 1. Selected bond lengths and angles for compound **1**–**8** are listed in Tables S1–S8 in the Supporting Information. Crystallographic data for the structures have been deposited in the Cambridge Crystallographic Data Centre; CCDC 745279 for **1**, CCDC 762972 for **2**, CCDC 763023 for **3**, CCDC 745282 for **4**, CCDC 763021 for **5**, CCDC 776676 for **6**, CCDC 776674 for **7**, and CCDC 776675 for **8** contain the supplementary crystallographic data for this paper. These data can be obtained free of charge from the Cambridge Crystallographic Data Centre via www.ccdc.cam.ac.uk/data_request/cif.

RESULTS AND DISCUSSION

Synthesis. Complexes **1**–**8** were synthesized by hydrothermal reaction under the same reaction temperature and time. The self-assembly reactions of $Na_2MoO_4\cdot 2H_2O$, H_3PO_4, TM^{2+}, $MCl_2\cdot 6H_2O$ (M = Ca, Sr, Ba), H_2O, and rigid organic ligands were carried out under similar conditions. The formation of basketlike $\{P_6Mo_{18}O_{73}\}$-based POM of this study relies on the presence of alkaline-earth-metal cations, which play the important template role for the assembly of the basketlike cages, and a series of similar reactions but without these cations resulted in simple $[P_4Mo_6]$-based POM or no crystals could be obtained. Here, we further explore the influence of different alkaline-earth-metal cations by using same organic agent bpy and transition-metal centers Cu^{2+} under the same hydrothermal conditions (see Scheme 1). The isostructural compounds **6**–**8** were prepared with the introduction of Ca^{2+}, Sr^{2+}, and Ba^{2+}. This indicates that these large ions are appropriate template reagent for the formation of the cryptate polyoxoanion $\{P_6Mo_{18}O_{73}\}$ and the difference of template reagent has not influence on the structural configurations of basketlike hybrid frameworks under similar conditions in our case. Unfortunately, if $MgCl_2$ was introduced into this system, no crystals could be obtained. The reason for which may be that the smaller size of Mg^{2+} cation and the shorter bond lengths of Mg–O cannot lead to the typical cagelike $\{P_6Mo_{18}O_{73}\}$ unit. In addition, basketlike crystals were found to be sensitive to the pH value and reaction temperature, which were controlled strictly at pH 3.0–4.0 and a reaction temperature of 160 °C, and no crystals could be obtained outside these pH ranges and reaction temperature.

dx.doi.org/10.1021/ic302311q | Inorg. Chem. 2013, 52, 485–498

At the beginning, the mixture of $Na_2MoO_4{\cdot}2H_2O$, H_3PO_4, $CuCl_2$, phen, and $SrCl_2$ in water at 160 °C for 4 days resulted in the first basketlike inorganic−organic hybrid compound **9**[10b] (see Scheme 2). This enlightened us to change the ligand to

Scheme 2. Illustration of the Relationship between Basket-Type Crystalline Structures and Different Rigid Organic Ligands and/or Transition Metals

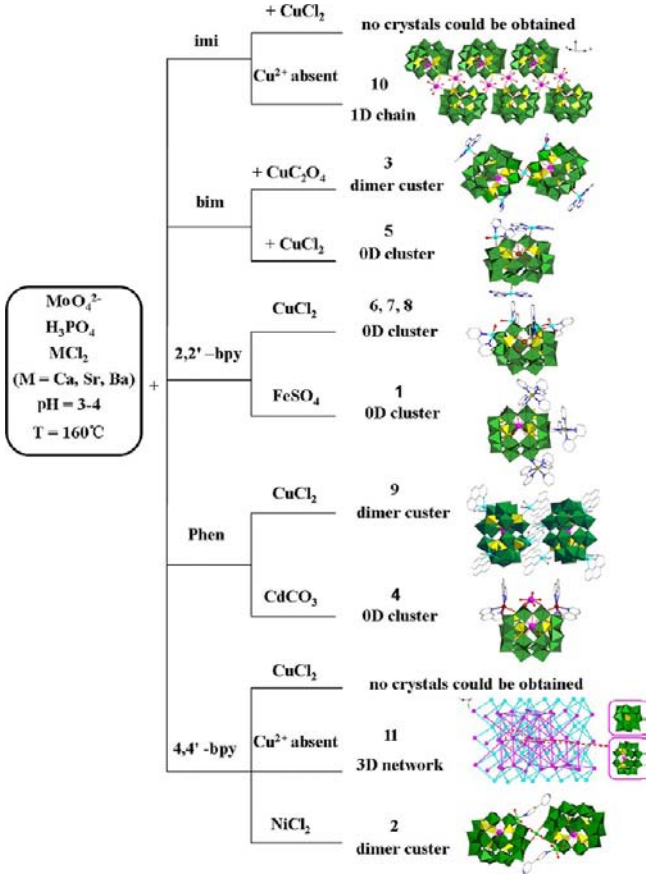

construct new hybrid supramolecular network under similar conditions. Unfortunately, when imi and 4,4′-bpy was used, no suitable crystal was obtained. However, when there is an absence of $CuCl_2$ under similar conditions, the first 1D assemblies of basket-type POMs $(H_2imi)_6(Himi)_4\{[Sr(H_2O)_4]_2[SrC{\subset}P_6Mo^{V}_4Mo^{VI}_{14}O_{73}]_2\}{\cdot}17H_2O$ (**10**)[10d] and a novel supramolecular 3D network based on the Keggin cluster and basketlike cage $(C_{10}H_{10}N_2)_{12}(PMo^{VI}_{12}O_{40})_2(SrC{\subset}P_6Mo^{V}_3Mo^{VI}_{15}O_{73})_2{\cdot}9H_2O$ (**11**)[14] were successfully isolated. When phen was replaced by bim or 2,2′-bpy, another two new 0D clusters (compounds **5** and **7**) were obtained. While both phen and $CuCl_2$ were substituted by bim and CuC_2O_4, respectively, compound **3** containing dimeric configuration was harvested. Furthermore, we tried to synthesize a series of basketlike hybrids containing the above organic units and other transition-metal centers, but it is a pity that only three types of supramolecular networks with Fe, Ni, and Cd (for compounds **1**, **2**, and **4**, respectively) were obtained. These results demonstrated that the different organic amines and transition metal have a significant structure-directing effect on the formation of the different extended basketlike frameworks. The formations of these complexes are shown in Scheme 2. Coordination modes of compounds **1**−**10** are summarized in Table 2. From the table, we can see that the coordination of the $\{P_6Mo_{18}\}$ heteropolyanion to metal ions mostly occurs at the oxygen atoms from four external phosphates and four molybdates of the handle of the "basket". Moreover, only three compounds (compounds **3**, **5**, and **9**) can coordinate to the terminal or bridged oxygen from $\{MoO_6\}$ octahedron of the "basket body" positions. Therefore, most active positions are located on one side of the "basket". Moreover, larger steric hindrance of basket POM itself leads to the current basketlike compounds formed only 0D monomers and dimer clusters or a one-dimensional dimer chain. Although basketlike compounds decorated by different rigid ligands and metal center exhibit interesting supramolecular frameworks from 1D to 3D via hydrogen bond interactions, the synthesis and exploration of high-dimensional covalent organic−inorganic hybrids based on basket-type POM still remains a great challenge to us.

Structure Description. X-ray diffraction (XRD) analysis reveals that the structures of compounds **1**−**8** contain the similar mixed-valent $\{MC{\subset}P_6Mo^{V}_nMo^{VI}_{18-n}O_{73}\}^{(6+n)-}$ (M = Ca, Sr, Ba; n = 2, 3, or 4) polyoxoanion, in which a tetravacant γ-Dawson-type $\{P_2Mo_{14}\}$ unit and a handle-shaped $\{P_4Mo_4\}$ unit are linked via the edge- and/or corner-sharing modes (see Figures 1a and 1d). The $\{P_4Mo_4\}$ unit consists of four $\{MoO_6\}$ octahedra and four $\{PO_4\}$ tetrahedra, which are corner-linked together to form the "handle" of the basket (Figure 1b). The "basket body" of the $\{P_2Mo_{14}\}$ block is derived from the γ-Dawson anion by the removal of four adjacent $\{MoO_6\}$ octahedral in the belt region (Figure 1c). The Mo−O bond lengths are within the range of 1.660(10)−2.441(3) Å, and the O−Mo−O bond angles vary from 84.9(4)° to 175.28(12)°. The P−O bond lengths are within the range of 1.471(13)−1.615(12) Å, and the O−P−O bond angles vary from 106.70(15)° to 115.12(17)° (see Tables S1−S6 in the Supporting Information). The entire basket-shaped cluster possesses $C2v$ symmetry (see Figure 1a). In the central cavity of the polyoxoanion, a M^{2+} ion (Ca^{2+} for **5** and **6**, Sr^{2+} for **1**, **2**, **3**, **4**, and **7**, Ba^{2+} for **8**) is fully encapsulated, exhibiting nine-/eight-coordination environment with the bond lengths of Ca−O in the range of 2.488(5)−2.625(7) Å, Sr−O in the range of 2.570(7)−2.754(6) Å, and Ba−O in the range of 2.643(6)−2.982(8) Å. It is proved that the cavity size of the basket-like polyoxoanion inclined to capture larger alkali metals or alkaline-earth cations. In fact, the incorporation of these large cations, conversely, may stabilize the entire cryptand polyoxoanion.

Structure of Compound 1. Compound **1** consists of one four-electron reduced $\{SrC{\subset}P_6Mo^{V}_4Mo^{VI}_{14}O_{73}\}^{10-}$ polyoxoanion, three isolated $\{Fe(2,2'\text{-bipy})_3\}$ fragments, and lattice water molecules (see Figure 2a and Figure S1 in the Supporting Information). The basketlike unit is a discrete cluster. There are three types of crystallographically independent Fe^{3+} cations, which exhibit the similar coordination environments in compound **1**. All Fe atoms exhibit an octahedral coordination environment, with six N atoms from three 2,2′-bpy ligands. The Fe−N bond lengths range from 1.950(5) Å to 1.983(5) Å, and the N−Fe−N bond angles vary from 81.2(2)° to 174.4(2)°. In compound **1**, the iron coordination complexes have a dual role: charge-balance and structure direction via hydrogen bands or supramolecular interactions. The adjacent polyoxoanion clusters are aggregated together via supramolecular interactions between C atoms of $\{Fe(1)(2,2'\text{-bpy})_3\}$ fragments and terminal O atoms of basket-type anion to form 1D chains (Figure 2b). The chain is further arranged in "ABAB..." manner through means of hydrogen bonds (O5W···O48, 3.083(9) Å;

dx.doi.org/10.1021/ic302311q | Inorg. Chem. 2013, 52, 485−498

Table 2. Illustration of the Relationship between Basket-Type Crystalline Structures and Different Rigid Organic Ligands and/or Transition Metals

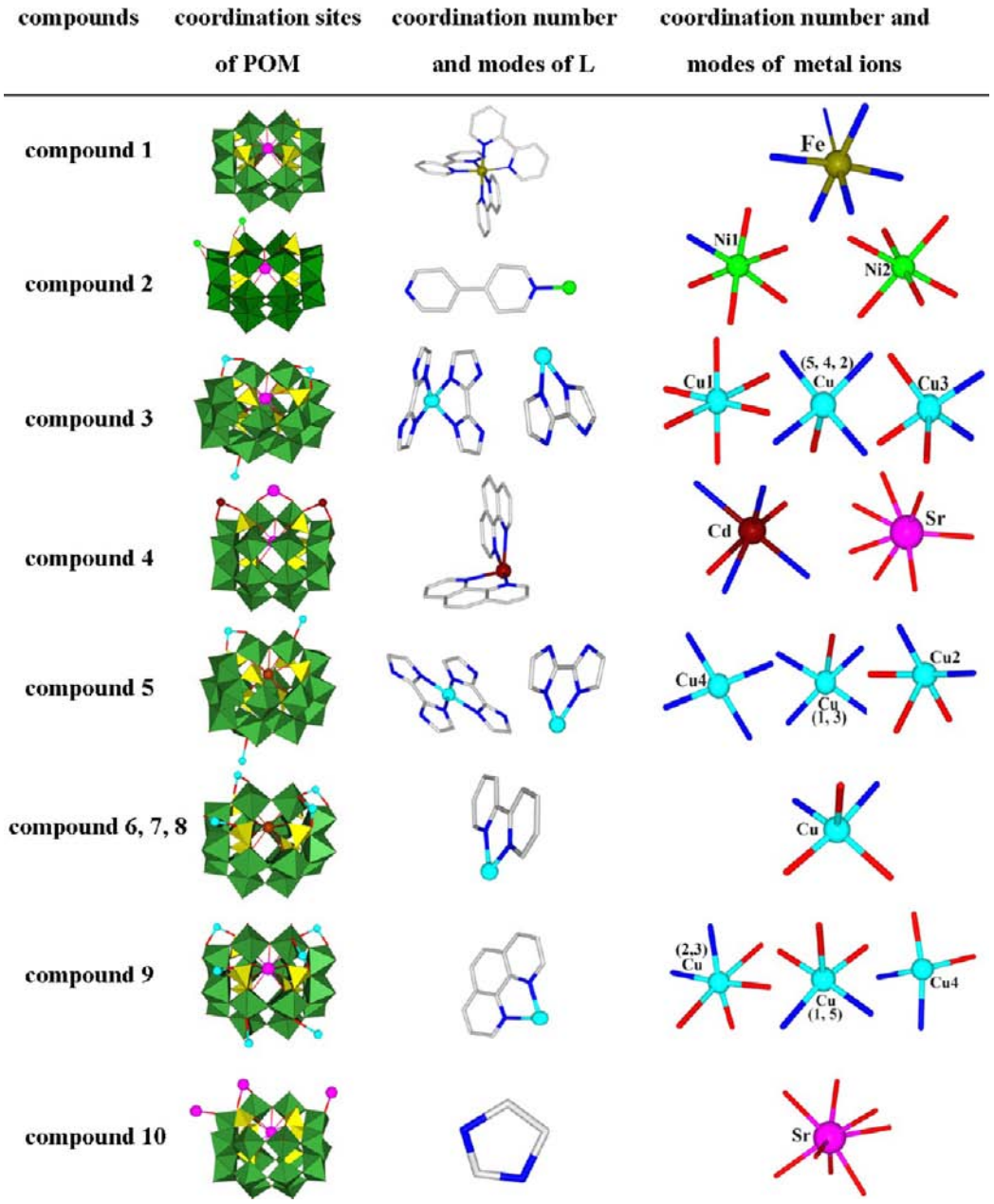

O5W···O71, 3.155(11) Å; and O5W···O5W, 2.969 Å) and supramolecular interaction (C23···O66, 3.037 Å; and C5···O66, 3.064 Å), giving birth to an infinite supramolecular double chain (see Figure 2c). The isolated water molecules link the double chains into the 2D supramolecular layer through four pairs of hydrogen bonds (see Table S7 in the Supporting Information). Each $\{Fe(1)(2,2'\text{-bpy})_3\}$ fragment connects three basketlike anions, and each basketlike anion links three $\{Fe(1)(2,2'\text{-bpy})_3\}$ fragments, meaning that each basketlike anion connected to five adjacent basket-type clusters through $\{Fe(1)(2,2'\text{-bpy})_3\}$ groups and water molecules to generate the 2D layers. Moreover, these adjacent 2D layers are further supported by similar supramolecular interaction to yield extending the 3D network structure (see Figure 2d). The typical supramolecular interactions are O30···C75, 3.125 Å and O24···C28, 3.216 Å. All the cationic $\{Fe(2,2'\text{-bpy})_3\}^{3+}$ units and solvent water molecules reside in the interspaces between two adjacent supramolecular layers.

Structure of Compound 2. Compound **2** is composed of 2 bielectron reduced polyoxoanion $\{Sr\subset P_6Mo^{V}_2Mo^{VI}_{16}O_{73}\}_2$ clusters, 2 $\{Ni(4,4'\text{-bipy})(H_2O)_3\}$ fragments, 1 $\{Ni(H_2O)_2\}$ linker, 5 protonated 4,4′-bipy, and 12 lattice water molecules (see Figure 3a and Figure S2 in the Supporting Information). According to the coordination environments, there are two different types of Ni^{2+} cations in **2**. Each Ni(1) cation forms a distorted octahedral configuration with nitrogen donors from 4,4′-bpy ligands (Ni(1)–N(6) = 2.077(15) Å), three oxygen donors from a coordinated water molecule, and two terminal oxygen atoms from one external phosphate and one molybdate of the handle of the "basket", respectively. The Ni(2) displays a slightly distorted octahedral coordination environment, which is defined by four oxygen atoms (O(59), O(63), and its

dx.doi.org/10.1021/ic302311q | Inorg. Chem. 2013, 52, 485−498

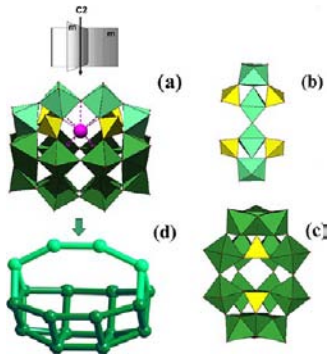

Figure 1. (a) Polyhedral and ball-and-stick representation of $[M\subset P_6Mo_{18}O_{73}]^{n-}$ (M = Ca, Sr, and Ba; n = 8, 9, and 10) polyoxoanion; (b) view of the "handle" $\{P_4Mo_4\}$ unit; (c) view of the "basket body" $\{P_2Mo_{14}\}$ unit; and (d) the basketlike topology formed by 18 Mo atoms.

symmetry related one) from two adjacent basketlike clusters and two oxygen donor from coordinated water molecule. The Ni–O distances are in the range of 2.053(13)–2.186(14) Å. The N–Ni–O and O–Ni–O angles are in the range of 89.2(5)°–174.6(6)° and 84.46°–180.0(5)°, respectively. Based on such connection modes, each nickel complex $\{Ni(bpy)(H_2O)_3\}^{2+}$ is bonded to two terminal oxygen atoms of basketlike anion to form a single-arm structure. Two adjacent monosupported structures are linked by Ni(2) atom to form dimeric cluster (Figure 3a). The adjacent dimeric units are bonded together by single-armed $\{Ni(bipy)(H_2O)_3\}^{2+}$ complexes and water molecule to form infinite 1D dimeric chains in ABAB mode via hydrogen bonds (O5W···O2, 3.010(17) Å and O5W···O58, 2.928(18) Å in Table S8 in the Supporting Information) and supramolecular interaction (N7···O44, 2.610 Å) (Figure 3b). The adjacent dimeric chains are further aggregated together to yield a 2D supramolecular layer in ABAB mode via protonated 4,4′-bipy with supramolecular interaction (N4···O62, 2.780 Å and N5···O48, 2.830 Å) (Figure 3c). The 3D supramolecular framework (Figure 3d) was generated by supramolecular interaction between different 2D layers with supramolecular interaction (O2W··· O52, 2.81(2) Å and O2W··· O76, 2.753 Å).

Structure of Compound 3. Compound **3** is three-electron-reduced type structure and displays similar dimeric clusters. The basic units of compound **3** consists of two basketlike $\{Sr\subset P_6Mo^{V}_3Mo^{VI}_{15}O_{73}\}^{9-}$ polyoxoanions decorated with $\{Cu(bim)_2\}$ and $\{Cu(bim)(H_2O)\}_2$ fragments, one $\{Cu(H_2O)_2\}$ linker and two $\{Cu_2(bim)_4(H_2O)\}$ counterions (see Figure 4a and Figure S3 in the Supporting Information). There are five crystallographically independent Cu atoms in compound **3**. The Cu(3) atom is pentacoordinated by two N atoms from one bim ligand and three O atoms, one of which are from water molecules, while the other two is from one external $\{PO_4\}$ and one $\{MoO_6\}$ octahedra of the handle of the "basket", respective. The Cu(5) atom is also pentacoordinated by four N atoms from two bim ligands and one *u*-O atom from $\{MoO_6\}$ octahedron of the "basket body" positions. In the $\{Cu_2(bim)_4(H_2O)\}$ charge-balanced unit, the Cu(2) and Cu(4) are bonded with four nitrogen atoms from two bim ligands and one *u*-O atoms of water molecules. It is noteworthy that two bisupported polyoxoanions are linked by $\{Cu1(H_2O)_2\}$ units to form a dimeric cluster (see Figure 4a). Cu(1) atom is octahedrally coordinated by two water molecules and four oxygen atoms (O(60), O(64), and its symmetry-related one) from two adjacent basketlike anions. The distances of Cu–O and Cu–N are in the range of 1.893(3)–2.404(4) Å and 1.975(4)–2.035(5) Å, respectively. The adjacent dimeric clusters are stably packed together by $\{Cu_2(bim)_4(H_2O)\}$ group and exhibit 1D supramolecular dimeric chains in ABAB mode with hydrogen bonds (N10···O41, 2.665(5) Å; N19···O66, 2.931(7) Å; and N20···O60, 3.040(6) Å) (see Figure 4b). The $\{Cu(5)(bim)(H_2O)\}$ fragments link the 1-D dimeric chains into the 2D supramolecular layer through a pair of hydrogen bonds (N2···O74, 2.912(6) Å). Moreover, these adjacent 2D layers are further linked together by hydrogen bonds N23···O7: 2.685(5) Å and N24···O2: 2.783(5) Å to lead to extending the 3D structure. It is striking that the structure of compound **3** exhibits extensive hydrogen-bonding interactions among polyoxoanions, Cu-bim groups, and lattice water molecules. The typical hydrogen bonds between them are as

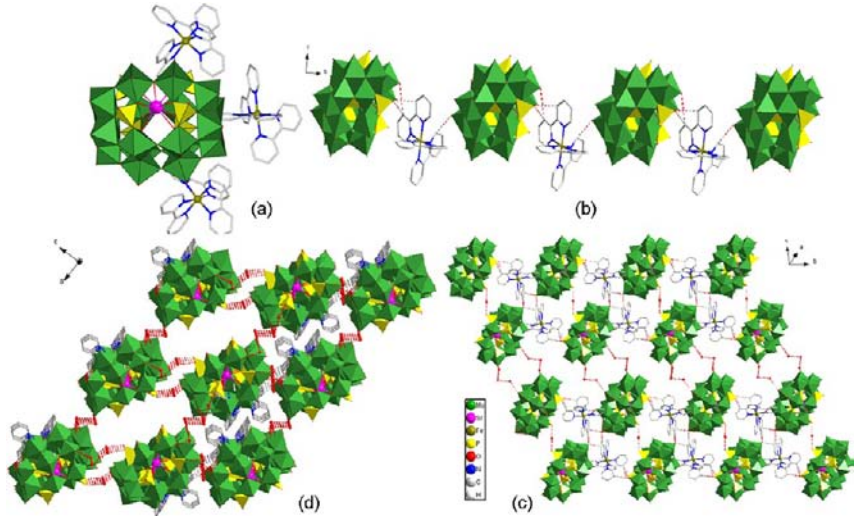

Figure 2. (a) The basic building unit of compound **1**; (b) the 1D chain of compound **1** based on $\{P_6Mo_{18}\}$ units and $\{Fe(2,2'\text{-bpy})_3\}$ linkers via supramolecular interactions; (c) the 2D supramolecular layer in compound **1**; and (d) the 3-D supramolecular network on the *ac*-plane of compound **1**.

dx.doi.org/10.1021/ic302311q | *Inorg. Chem.* 2013, 52, 485–498

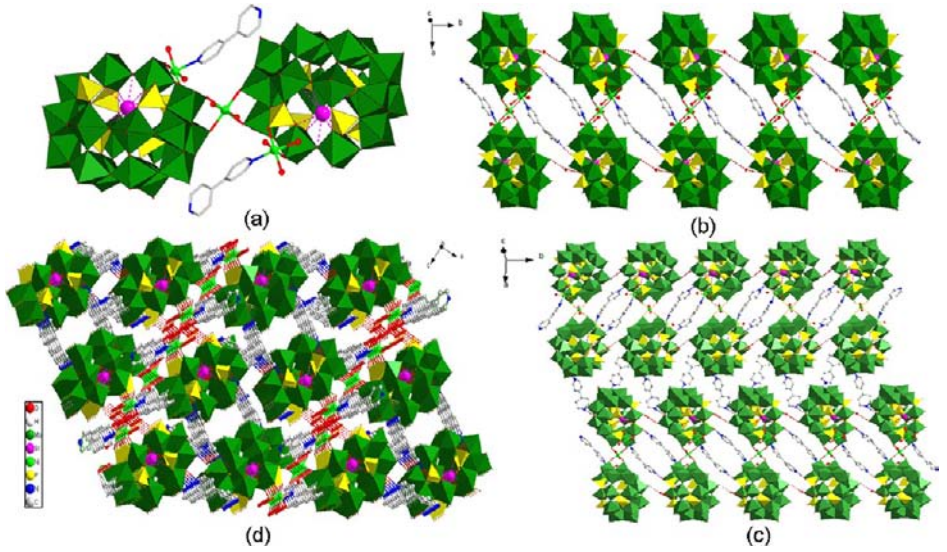

Figure 3. (a) The dimeric cluster of compound **2**; (b) the 1D demeric chain of compound **2** based on $\{P_6Mo_{18}\}$ units and $\{Ni(4,4'\text{-bpy})(H_2O)_3\}$ linkers in ABAB mode via hydrogen bonds and supramolecular interactions; (c) the 2D supramolecular layer in ABAB mode in compound **2**; and (d) the 3D supramolecular network on the *ac*-plane of compound **2**.

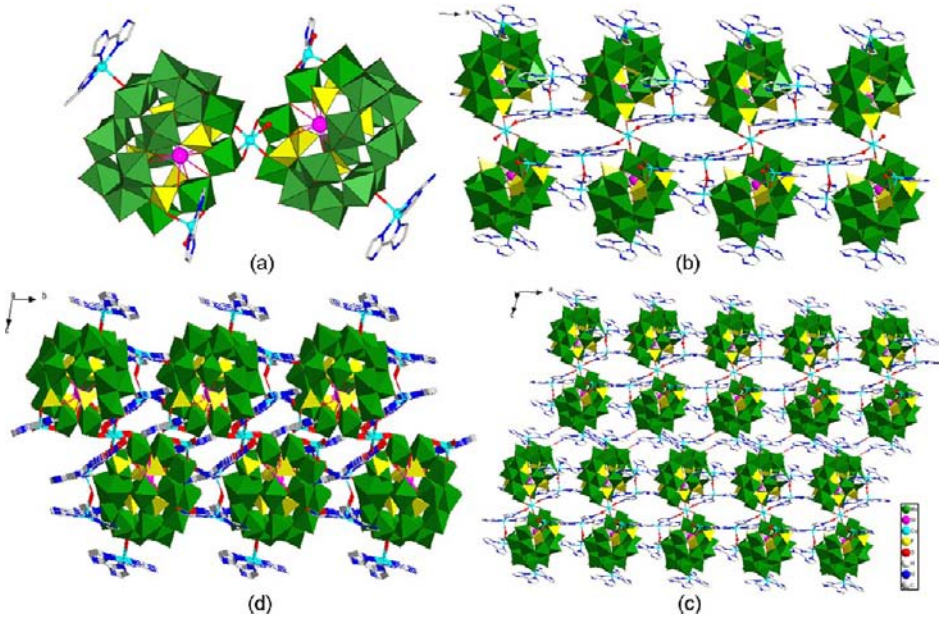

Figure 4. (a) The dimeric cluster of compound **3**. (b) The 1D dimeric chain of compound **3**, based on $\{P_6Mo_{18}\}$ units and $\{Cu_2(bim)_4(H_2O)\}$ linkers in ABAB mode via hydrogen bonds interactions. (c) The 2D supramolecular layer in ABAB mode in compound **3**. (d) The 3D supramolecular network in ABAB on the *bc*-plane of compound **3**.

follows: O63···O5W, 3.181(6) Å; O5W···N20, 3.134(6) Å; N16···O29, 2.806(5) Å; N15···O56, 2.696(5) Å (as shown in Table S9 in the Supporting Information).

Structure of Compound 4. Compound **4** represents a four-electron-reduced bisupported structure when changing transition-metal cations under similar conditions. Compound **4** consists of a $\{SrCP_6Mo^{V}_4Mo^{VI}_{14}O_{73}\}^{10-}$ polyoxoanion modified by two $\{Cd(phen)_2\}^{2+}$ complexes and one $\{Sr(H_2O)_5\}$ cation, and lattice water molecules (Figure 5a and Figure S4 in the Supporting Information). Two $\{Cd(phen)_2\}^{2+}$ complexes are coordinated with two terminal phosphate−oxygen and two molybdate−oxygen atoms from two symmetrical "handle" positions of a basketlike anion. The bond lengths of Cd−N and Cd−O are in the range of the 2.333(12)−2.369(14) and 2.223(10)−2.573(10) Å, respectively. It is very interesting that one Sr(1) atom linked to a basketlike polyoxoanion by two terminal O atoms from two symmetrical $\{MoO_6\}$ octahedra in the middle of "handle" positions. Five oxygen atoms from water molecules completes the coordination sphere of the Sr1 centers, the Sr1−O distances are 2.189(14)−2.43(3) Å. It is noteworthy that each $[SrCP_6Mo^{V}_4Mo^{VI}_{14}O_{73}]^{10-}$ unit acts as a hexadentate ligand coordinating to two $\{Cd(phen)_2(H_2O)\}$ and one $Sr(H_2O)_5$ subunits via the terminal O atoms of one side of the basketlike units to generate a unique asymmetric bisupported structure. Because two $\{Cd(phen)_2(H_2O)\}$ and a $\{Sr(H_2O)_5\}$ units are located on one side of the "basket", the larger steric hindrance restricts the formation of dimeric clusters. However, the coordination water of the Sr ion can

dx.doi.org/10.1021/ic302311q | *Inorg. Chem.* 2013, 52, 485−498

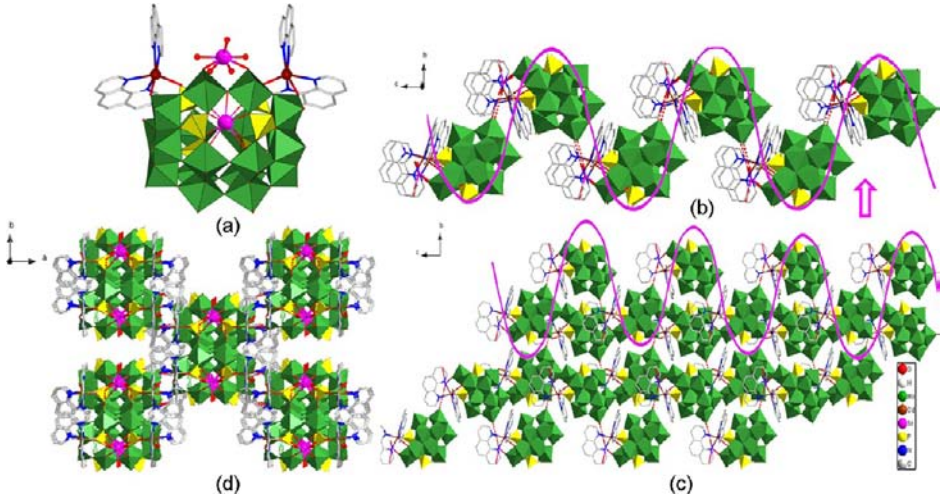

Figure 5. (a) The basic building unit of compound **4**. (b) The 1D zigzag chain of compound **4** based on $\{P_6Mo_{18}\}$ units and $\{Cd(phen)_2\}$ linkers via hydrogen bonds interactions. (c) The 2D supramolecular layer in compound **4**. (d) The 3D supramolecular network on the *ab*-plane of compound **4**.

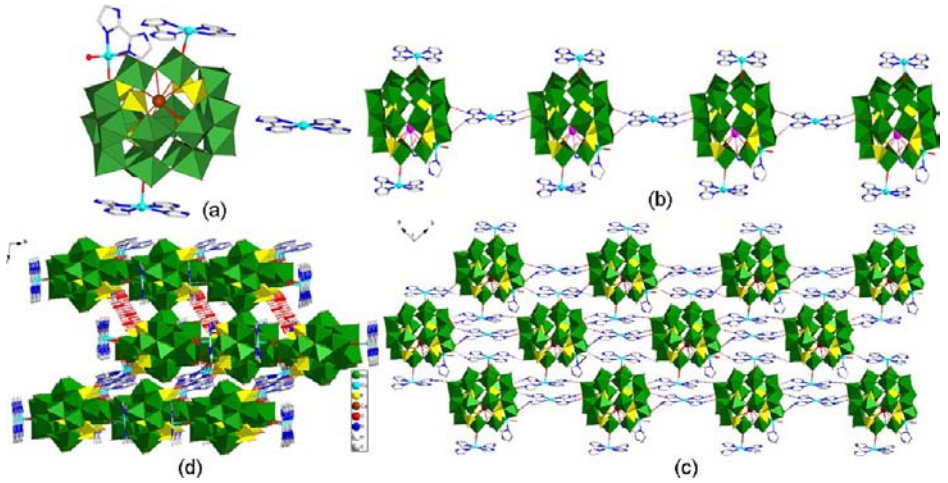

Figure 6. (a) The basic building unit of compound **5**. (b) The 1D straight chain of compound **5** based on $\{P_6Mo_{18}\}$ units and $\{Cu(4)(bim)_2\}^{2+}$ linkers via hydrogen bonds interactions. (c) The 2D supramolecular layer in compound **5**. (d) The 3D supramolecular network in ABAB mode on the *ac*-plane of compound **5**.

interact with terminal O atoms of adjacent polyoxoanion via hydrogen bonds (O40···O22, 2.84(2) Å, as shown in Table S10 in the Supporting Information) to form a zigzag chain. Adjacent chains are linked together to form a 2D layer and a 3D framework by supramolecular interaction between C atoms of phen groups and O atoms of polyoxoanion (Figures 5c and 5d) The typical interaction between them are as follows: C15···O23, 3.045 Å; C4···O21, 3.021 Å; C8···O39, 2.985 Å; and C5···O21, 2.952 Å.

Structure of Compound 5. The building units of compound **5** are composed of one three-electron-reduced $\{CaC\subset P_6Mo^{V}_3Mo^{VI}_{15}O_{73}\}^{9-}$ polyoxoanions, two $\{Cu(bim)_2\}$ fragment, one $\{Cu(bim)(H_2O)_2\}$ complex, one $\{Cu(bim)_2\}^{2+}$ counterion, and nine lattice water molecules (see Figure 6a and Figure S5 in the Supporting Information). It is noteworthy that each $\{CaC\subset P_6Mo^{V}_3Mo^{VI}_{15}O_{73}\}^{9-}$ cluster unit acts as a tetradentate ligand coordinating to two $\{Cu(bim)_2\}$ and a $\{Cu(bim)(H_2O)_2\}$ subunit via terminal O atoms of the anion to generate the trisupported structures (Figure 6a). There are four crystallographically independent Cu-bim complexes that have different coordination environments. The Cu(1) and Cu(3) atoms are pentacoordinated, in which Cu(1) center is coordinated with four N atoms from two bim ligand and one *u*-O atom from $\{MoO_6\}$ octahedra of "basket-body" positions. The Cu(3) atom is also defined by four N atoms of two bim ligands and a terminal O atom from $\{MoO_6\}$ octahedra of the "handle" positions. The Cu(2) atom is in the center of a distorted octahedron, which is bonded to two N atoms of bim, a terminal P−O and molybdate−oxygen atoms from the "handle" positions of the polyoxoanion, and two water molecules. The Cu(4) atom is coordinated to four N atoms of two bim ligands, which isolated in the interspace of the crystal structure as counterion. The bond lengths of Cu−N and Cu−O are in the range of the 1.976(4)−2.054(4) Å and 1.938(3)−2.409(3) Å, respectively. The isolated $\{Cu(4)(bim)_2\}^{2+}$ cations link the basketlike anion to an infinite 1D straight chain through four pairs of hydrogen bonds interactions (N4···O66, 2.980(5) Å; N2···O69, 2.950(5) Å; N6···O34, 2.777(5) Å, and N7···O47, 2.850(5) Å) (Figure 6b). These 1D chains are parallel with each other and further link two adjacent identical ones to generate 2D supramolecular layer through $\{Cu(1)(bim)_2\}^{2+}$ linker with hydrogen bonds

dx.doi.org/10.1021/ic302311q | *Inorg. Chem.* 2013, 52, 485−498

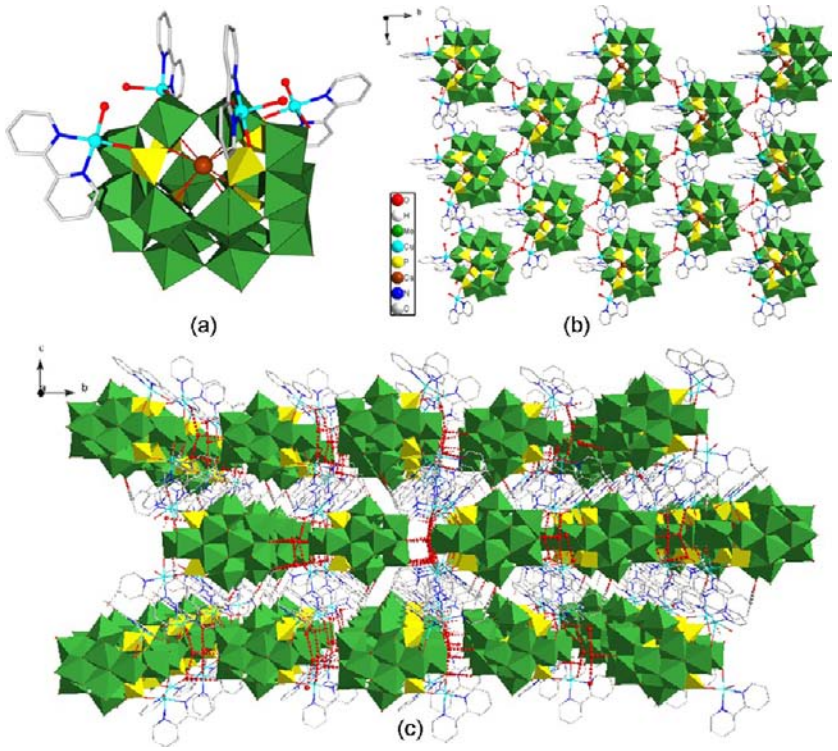

Figure 7. (a) The basic building unit of compound **6**. (b) The 2D supramolecular layer in compound **6**. (c) The 3D supramolecular network in ABAB mode on the *bc*-plane of compound **6**.

interactions (N25···O64, 2.867(5) Å and N28···O72, 3.074(6) Å) (Figure 6c). The adjacent 2D layers are linked together to form a 3D supramolecular network in ABAB mode via strong hydrogen-bonding and supermolecular interactions (Figure 6d). The typical hydrogen bonds are N11···O36, 2.798(5) Å and N12···O36, 2.978(6) Å (see Table S11 of the Supporting Information). The supermolecular interactions are as follows: O6W···O57, 2.991 Å; O7W···O6W, 2.814 Å; and O7W···O70, 3.025 Å.

Structure of Compounds 6, 7, and 8. Compounds **6**, **7**, and **8** are isostructural tetrasupported structures with only slight differences in guest ions and the number of lattice waters. They are constituted of a two-electron-reduced $[M\subset P_6Mo^{V}_2Mo^{VI}_{16}O_{73}]^{8-}$ (M = Ca for **6**, Sr for **7**, and Ba for **8**) polyoxoanion decorated with four {Cu(bpy)(H_2O)}, and water molecules (see Figure 7a and Figure S6 in the Supporting Information). There are four independent {Cu(2,2′-bpy)-(H_2O)} fragments that are coordinated to the surface of the polyoxoanion directly. All of the Cu atoms of these compounds exhibit a five-coordinate environment with a terminal P−O, molybdate−oxygen atoms from the "handle" position of the polyoxoanion, two N atoms from the 2,2′-bpy ligand, and one water ligand. The bond lengths of Cu−N are within the range of 1.972(7)−1.999(6) Å in compound **6**, 1.960(16)−2.025(14) Å in compound **7**, and 1.957(8)−2.006(7) Å in compound **8**. The bond lengths of Cu−O are within the range of 1.907(5)−2.237(7) Å in compound **6**, 1.910(12)−2.210(14) Å in compound **7**, and 1.903(6)−2.184(8) Å in compound **8**. Each polyoxoanion cluster is connected to four other coplanar anions via three pairs of hydrogen bonds (O3W···O41, 2.910(18) Å; O3W···O39, 3.031(18) Å; and O41···O33, 3.445 Å, shown in Table S12 in the Supporting Information) to form a 2D layer (Figure 7b). Supermolecular interactions between carbon atoms of {Cu(1)(bpy)(H_2O)} and terminal oxygen atoms of polyanions are also found to stabilize the 3D supramolecular framework (Figure 7c). The typical supermolecular interactions are C16···O9, 3.179 Å and C8···O26, 3.157 Å.

Bond-valence sum (BVS) calculations[15] show an average value of ca. 5.79 for Mo centers in compound **1** and **4** (see Tables S13 and S16 in the Supporting Information), which is close to the result of 14 Mo^{6+} and 4 Mo^{5+} in the polyoxoanion cluster. The BVS results are ∼5.81 for Mo centers in compound **3** and **5** (see Tables S15 and S17 in the Supporting Information), indicating that their oxidation states are 15 Mo^{6+} and 3 Mo^{5+} in the polyoxoanion. BVS calculations display average value of ca. 5.86 for Mo centers in compound **2** (Table S14 in the Supporting Information) and 5.88 for that in compounds **6**, **7**, and **8** (BVS results of compounds **6**, **7**, and **8** are very similar for their isomorphism; the value of compound **7**, for example, is shown in Table S18 in the Supporting Information), which is about the result of 16 Mo^{6+} and 2 Mo^{5+} in the polyoxoanion. In addition, BVS calculations confirm that all P centers are in the oxidation states of +5, and Cu centers in compound **3**, **5**, **6**, **7**, and **8**, Cd centers in compound **4**, Ni centers in compound **2**, Ca centers in compounds **5** and **6**, Ba centers in compound **8**, and Sr centers in compounds **1**, **2**, **3**, **4**, and **7** are in the +2 oxidation state. BVS calculations also show that all Fe centers in compound **1** are in the +3 oxidation state. BVS shows that water ligands (O67) only bridged two $Cu(bim)_2$ complexes in compound **5** (BVS value is 0.32). Moreover, two, two, four, and one extra protons should be added to the lattice water molecules or organic agents in compounds **1**, **2**, **4**, and **5**, respectively, for the charge balance. Thus, compounds **1**−**8** can be formulated as described above.

IR Spectroscopy. The IR spectra of compounds **1**−**8** recorded between 400 cm^{-1} and 4000 cm^{-1} with KBr pellet (see Figures S7a−f in the Supporting Information) are similar:

dx.doi.org/10.1021/ic302311q | *Inorg. Chem.* 2013, 52, 485−498

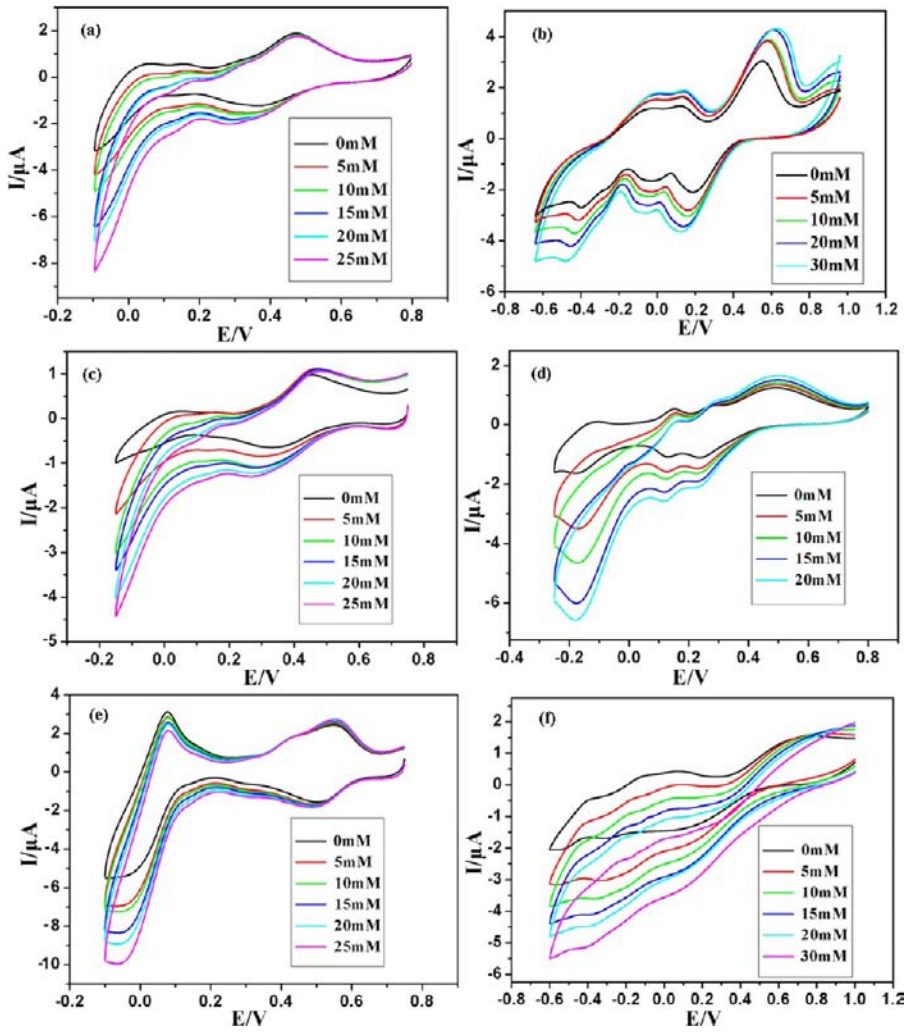

Figure 8. Cyclic voltammograms of (a) **1**, (b) **2**, (c) **3**, (d) **4**, (e) **5**, and (f) **6**-**CPE** in 1 M H_2SO_4 solution containing nitrite at different concentrations. (Potentials vs SCE. Scan rate = 30 mV s^{-1}.)

the peaks at 1180−1031 cm^{-1} are attributed to υ(P−Oa) vibrations; the strong peaks at 990−932 cm^{-1} are ascribed to υ(Mo=O terminal) vibrations; peaks at 841−760 cm^{-1} are assigned to v(Mo−O bridge) vibrations. The peaks located at 510−618 cm^{-1} can be attributed to υ(TM−O).[16a] The strong peaks at 1512−1421 cm^{-1} are indicative of υ(C−N) vibrations of organic ligands. Furthermore, the broad peaks between 3010 and 3484 cm^{-1} and the peaks at 1620−1654 cm^{-1} can be assigned to υ(N−H) and/or υ(O−H) of the protonated pyridine-containing ligands and water molecules.

UV Spectroscopy. In the UV spectras of compounds **1**−**8** (Figures S7a−f in the Supporting Information), the two strong bands in the range of 242−262 nm and 307−324 nm are attributed to (LMCT) $p\pi(O_{terminal})\rightarrow d\pi^*(Mo)$ electronic transitions in the Mo═O bonds and $d\pi-p\pi-d\pi$ electronic transitions between the energetic levels of the Mo−O−Mo bonds, respectively.[16a] The broad band at 602−640 nm ascribed to overlap of two bands of the intervalence transition from the Mo^V to Mo^{VI} via the Mo−O−Mo bond, the d−d transitions of Mo^V octahedral,[15a] and the $Cu-N_{(organic\ ligand)}$ and $Cu-O_{(POM)}$ LMCT bands,[16b] leading to the dark blue coloration of these compounds.

XPS Spectroscopy. The oxidation states of Mo are further confirmed by X-ray photoelectron spectroscopy (XPS) measurements, which were carried out in the energy region of Mo $3d_{5/2}$ and Mo $3d_{3/2}$ (see Figures S9a−f in the Supporting Information). The XPS spectrum of compounds **1**−**6** presents four overlapped peaks at 231.2−231.6 eV, 234.0−234.6 eV, 235.1−235.7 eV, and 232.3−232.6 eV in the Mo 3d region, which should be ascribed to the mixture of Mo^{5+} and Mo^{6+}, respectively.[16c] The XPS results also support the BVS calculations for the Mo oxidation states, in which the deconvolution of the spectra indicates that the ratio of Mo^{VI}/Mo^V is ∼7:2 for compounds **1** and **4**, ∼5:1 for compounds **3** and **5**, and ∼8:1 for compounds **2** and **6**.

TG Analyses. The thermal stabilities of compounds **1**−**8** were investigated under a N_2 atmosphere from 40 °C to 800 °C, and the TG curves are shown in Figure S10a−f in the Supporting Information. In the TG curve of compound **1**, the first weight loss of 2.46% (calcd 2.07%) at 189−340 °C corresponds to the loss of 11 lattice water molecules. The second weight loss, between 415 °C and 680 °C, of 28.85% arises from the loss of all 2,2′-bpy molecules (calcd 29.04%, for 18 bpy). For **2**, the first weight loss of 4.98% (calcd 4.51%) at 124−182 °C is attributed to 12 lattice water molecules and 8 coordinated water molecules in compound **2** (for 20 H_2O). The second and third weight losses of 14.50% at 345−680 °C correspond to the loss of 4,4′-bpy molecules (calcd 13.71%, for

dx.doi.org/10.1021/ic302311q | *Inorg. Chem.* 2013, 52, 485−498

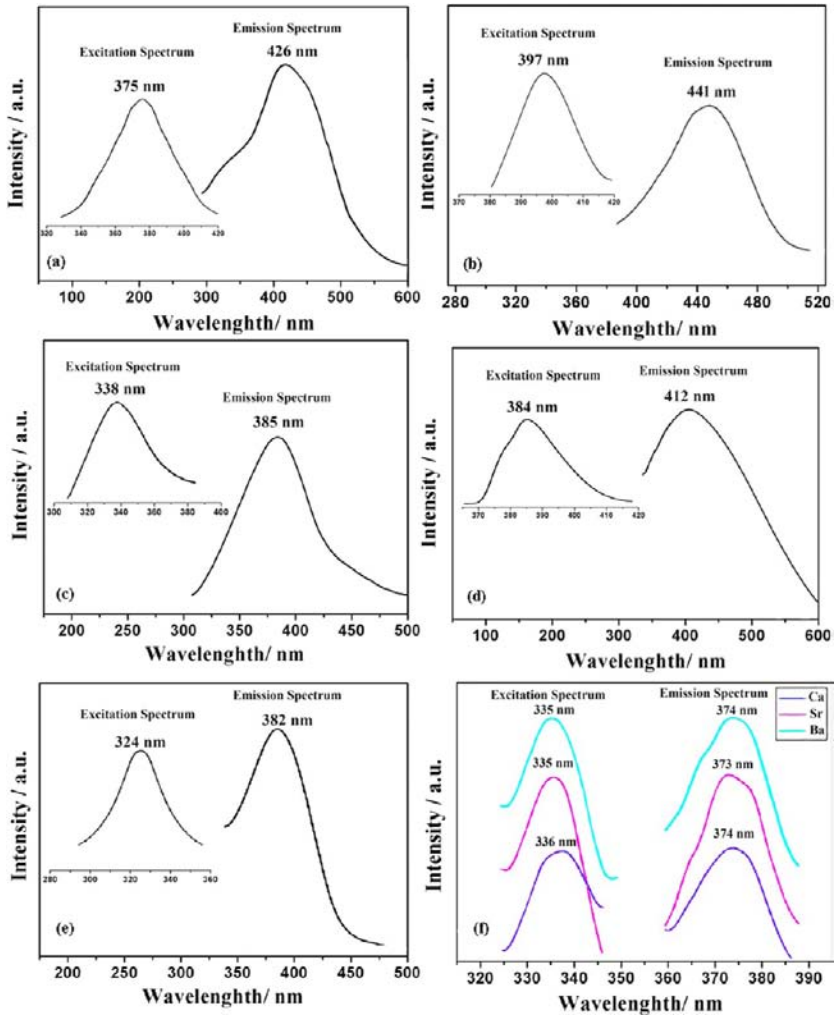

Figure 9. Fluorescent spectra of (a) compound **1**, (b) compound **2**, (c) compound **3**, (d) compound **4**, (e) compound **5**, and (f) Ca for compound **6**, Sr for compound **7**, and Ba for **8**.

7 bpy). For **3**, the first weight loss of 4.53% in the temperature of 120−285 °C is due to the loss of all lattice water molecules and coordinated water molecules in compound 3 (calculated value 4.32% for 22 H_2O). The second weight loss of 20.15% between 320 °C and 610 °C arises from the loss of bim organic ligands. The value is close to the calculated value of 20.45% (for 14 bim). For **4**, the first weight loss of 4.76% at 148−210 °C corresponds to the loss of discrete water and coordinated water molecules (calcd 4.20%, for 7 H_2O). The second weight loss between 210 and 502 °C of 15.92% relates from the evacuation of all phen molecules (calcd 16.44%, for 4 phen). The TG curves of compound **5** exhibits three steps weight loss: the first weight loss of 4.82% (calcd 4.39%) at 126−232 °C corresponds to the loss of lattice water and coordinated water molecules. The second and third weight losses, between 374 °C and 678 °C, of 21.62% arise from the loss of all of the bim molecules (calcd 20.86%). The TG curves of compounds **6**, **7**, and **8** exhibit three steps of weight loss: the first weight loss of 2.95% (calcd 2.63%), 2.63% (calcd 2.56%), and 3.67% (calcd 3.39%)—at 29−151 °C, 56−150 °C, and 44−155 °C, respectively—arises from the discrete water molecules. The second weight loss of 14.95% (calcd 15.18%), 16.68% (calcd 15.01%), and 15.77% (calcd 14.71%) at 300−560, 320−575, and 350−545 °C, respectively, relates to the loss of 2,2′-bpy ligands on copper centers. The third weight loss of 8.74% (calcd 10.36%), 9.24% (calcd 10.24%), 9.45% (calcd 10.04%) corresponds to the loss of P_2O_5. All of the weight loss from the TG curves are consistent with the formulas of compounds **1**−**8**.

Electrochemical and Electrocatalytic Properties. Although compounds **1**−**8** were obtained from the aqueous system, they cannot be dissolved in water or acidic aqueous solutions; therefore, their electrochemical behavior was investigated with **1**-**6**-modified carbon paste electrode (**1**-**6**-**CPE**).[17] (The electrochemical behaviors of compounds **6**, **7**, and **8** are very similar for their isomorphism, so only compound **6** is shown as a example.) The cyclic voltammetric behavior of **1**-**6**-CPE in 1 M H_2SO_4 aqueous solution at different scan rates was recorded in the potential range from 1.0 V to −0.8 V (see Figure S11a in the Supporting Information). The cyclic voltammogram (CV) of **1**-**6**-**CPE** shows reversible redox peaks with the half-wave potentials of $E_{1/2} = (E_{pa} + E_{pc})/2$ at +0.42 V, +0.29 V, and +0.11 V for **1**, +0.36 V, +0.06 V, and −0.19 V for **2**, +0.41 V, +0.22 V, and +0.02 V for **3**, +0.51 V, +0.26 V, +0.16 V, and −0.14 V for **4**, +0.53 V, +0.25 V, and +0.04 V for **5**, +0.44 V, +0.12 V, and −0.26 V for **6**, respectively (based on the CV at 30 mV s^{-1}), which ascribed to three consecutive two-electron processes of substituted basket $[MCP_6Mo_{18}O_{73}]^{n-}$ heteropolymolybdate framework.[18] Although compounds **1**−**6** contain similar polyoxometallate anions, the mean peak potentials are slightly different, because

dx.doi.org/10.1021/ic302311q | *Inorg. Chem.* 2013, 52, 485−498

of their different chemical environments and the number of "blue" electrons. The cathodic peak potentials of all compounds **1**−**6** shift toward the negative direction and the corresponding anodic peak potentials shift to the positive direction with increasing scan rates, as shown in Figure S11 in the Supporting Information. The peak potentials change gradually following the scan rate from 20 mV s^{-1} to 500 mV s^{-1}. Moreover, the peak-to-peak separations between the corresponding anodic and cathodic peaks increased, but the average peak potentials do not change overall. The plots of anodic peak current (II) vs scan rates (see inset plots in Figure S11 in the Supporting Information) indicate that the redox processes of **1-6-CPE** are surface-controlled below the scan rate of 100 mV s^{-1}, while at scan rates higher than 100 mV s^{-1}, the peak currents were proportional to the square root of the scan rate, suggesting that redox processes are diffusion-controlled.[19] It is also noteworthy that **1-6-CPE** possesses high stability. When the potential range is maintained between −0.8 V and 1.0 V, the peak currents remains almost unchanged over 300 cycles at a scan rate of 100 mV s^{-1}. The high stability of **1-6-CPE** could be ascribed to the organic−inorganic hybrid structural feature of **1-6** that stabilizes the polyoxoanion in the compound.

Furthermore, **1-6-CPE** displays good electrocatalytic activity upon the reduction of nitrite (Figure 8). At the **1-6-CPE**, with the addition of $NaNO_2$, all reduction peak currents increased while the corresponding oxidation peak currents dramatically decreased, suggesting that $NaNO_2$ was reduced by all six reduced polyoxoanion species.[19] It has been noted that the shift of the two-reduced form (compounds **2** and **6**) is relatively weaker than the three- or four-reduced forms, which proved that the catalytic activities were enhanced with the increasing extent of the anion reduction.

Fluorescent Properties. The solid-state emission spectra of compounds **1**−**8** at room temperature are depicted in Figure 9. Compounds **1**, **6**, **7**, and **8** exhibit intense emissions maxima at ca. 426, 374, 373, and 374 nm, respectively (see Figure 9a, λ_{ex} = 375, 335, 335, and 336, respectively). According to the literature,[20] these emissions can be assigned to the emission of ligand-to-metal charge transfer (LMCT).[20] It is known that the free 2,2′-bpy molecule displays a weak luminescence at ca. 530 nm in the solid state at room temperature. The blue shifts and the luminescent enhancement compared to that of free 2,2′-bpy molecule may be due to the chelation of the 2,2′-bpy ligand to the metal ion, which effectively increases the rigidity of the ligand and reduces the loss of energy by radiationless decay of the intraligand emission excited state.[21] The emission spectra of compounds **6**−**8** are very similar, because they are isostructural and their ligands and transition metals are of the same types. It can also be observed that intense emissions occurring at 385, 412, 382 nm, respectively (Figures 9c−e, λ_{ex} = 338, 384, 324 nm, respectively) for compounds **3**, **4**, and **5**. According to previous observations,[22,23] these emission bands probably are assigned to the LMCT emission. The maximum emission band occurs at 453 nm upon excitation at 397 nm for **2** (Figure 9b). The peak at 441 nm is closed to the emissions band of free 4,4′-bpy ligand (437 nm) attributed to the intraligand emission from the protonated 4,4′-bpy ligand.[24] Paramagnetic nickel(II) is a good photoluminescence quencher reagent, which can lead to the fluorescent quencher of the organic ligand linked to it. Therefore, compound **2** only exhibits the intraligand emission instead of LMCT. These observations indicate that compounds **1**−**8** may be excellent candidates for use as photoluminescence materials.

CONCLUSION

In this paper, four types of rigid ligands (bim, 2, 2-bpy, 4,4-bpy, phen) have been used for construction of eight basket-based supramolecular compounds under hydrothermal conditions. Furthermore, transition metals Fe^{3+}, Ni^{2+}, and Cd^{2+} are first introduced into basketlike hybrid systems. In addition, as a new template reagent, the Ca^{2+} and Ba^{2+} cations are also first introduced into reaction systems, leading to the assembly of a basketlike POM. Electrochemical analysis shows that **1-6-CPE** displays unique redox properties and good electrocatalytic activity to reduce the nitrite. Furthermore, fluorescence analysis shows that all the title compounds are potential fluorescent-emitted materials. The ongoing efforts will be concentrated on the introduction of flexible ligands into the basket-type reaction systems, to get new high-dimensional covalent organic−inorganic hybrid materials and explore their property. Although the actual spatial dimension of basketlike POM is still very low (only 0D and 1D), the successful synthesis of compounds **1**−**8**, to some extent, provides useful prototypes for further research on basket-based organic−inorganic hybrid compounds.

ASSOCIATED CONTENT

Supporting Information

X-ray crystallographic files for compounds **1**−**8** in CIF format, 11 plots (the molecular structural unit, XPS, IR, and UV spectra, TG and cyclic voltammograms of compound curves (Figures S1−S11), and tables of selective bond lengths and bond angles, hydrogen bond lengths and bond angles, and bond valence sum calculations of Mo centers for **1**−**8** (Tables S1−S18). This material is available free of charge via the Internet at http://pubs.acs.org.

AUTHOR INFORMATION

Corresponding Author

*Tel.: (+86) 0451-88060173. E-mail: zhou_bai_bin@sina.com.

Notes

The authors declare no competing financial interest.

ACKNOWLEDGMENTS

This work is supported by the National Natural Science Foundation of China (Grants Nos. 20671026, 20971032, 20701005 and 21271056), the Natural Science Foundation of Heilongjiang Province (No. B201216), the Study Technological Innovation Project Special Foundation of Harbin (No. 2009RFXXG202), the Science and Technology Project of Education Office of Heilongjiang Province (No. 11551122), Key Laboratory of Functional Inorganic Material Chemistry (Heilongjiang University), Ministry of Education, Technological Innovation Team Building Program of College of Heilongjiang Province (No. 2009td04), and Innovation Team Research Program of Harbin Normal University (No. KJTD200902).

REFERENCES

(1) (a) Gouzerh, P.; Proust, A. *Chem. Rev.* **1998**, *98*, 77. (b) Getman, R. B.; Bae, Y. S.; Wilmer, C. E.; Snurr, R. Q. *Chem. Rev.* **2012**, *112*, 703. (c) Suh, M. P.; Park, H. J.; Prasad, T. K.; Lim, D. W. *Chem. Rev.* **2012**, *112*, 782. (d) Li, J. R.; Tao, Y.; Yu, Q.; Bu, X. H.; Sakamoto, H.; Kitagawa, S. *Chem.—Eur. J.* **2008**, *14*, 2771. (e) Long, D. L.; Burkholder, E.; Cronin, L. *Chem. Soc. Rev.* **2007**, *36*, 105. (f) Lydon, C.; Busche, C.; Miras, H. N.; Delf, A.; Long, D. L.; Yellowlees, L.; Cronin, L. *Angew. Chem., Int. Ed.* **2012**, *51*, 2115. (g) Zeng, Y. F.; Hu, X.; Liu, F. C.; Bu, X. H. *Chem. Soc. Rev.* **2009**, *38*, 469. (h) Horcajada,

P.; Gref, R.; Baati, T.; Allan, P. K.; Maurin, G.; Couvreur, P.; Férey, G.; Morris, R. E. C. Serre *Chem. Rev.* **2012**, *112*, 1232. (i) Yin, P.; Pradeep, C. P.; Zhang, B. F.; Li, F. Y.; Lydon, C.; Rosnes, M. H.; Li; Bitterlich, D. E.; Xu, L.; Cronin, L.; Liu, T. B. *Chem.—Eur. J.* **2012**, *18*, 8157. (j) Du, M.; Guo, Y. M.; Chen, S. T.; Bu, X. H.; Batten, S. R.; Ribas, J.; Kitagawa, S. *Inorg. Chem.* **2004**, *43*, 1287.

(2) (a) Burkholder, E.; Golub, V.; O'Connor, C. J.; Zubieta, J. *Inorg. Chem.* **2004**, *43*, 7014. (b) Pradeep, C. P.; Long, D. L.; Kögerler, P.; Cronin, L. *Chem. Commun.* **2007**, 4254. (c) Rieger, J.; Antoun, T.; Lee, S. H.; Chenal, M.; Pembouong, G.; Haye, J. L.; Azcarate, I.; Hasenknopf, B.; Lacôte, E. *Chem.—Eur. J.* **2012**, *18*, 3355. (d) Niu, J. Y.; Zhang, X. Q.; Yang, D. H.; Zhao, J. W.; Ma, P. T.; Kortz, U.; Wang, J. P. *Chem.—Eur. J.* **2012**, *18*, 6759. (e) Fu, H.; Li, Y. G.; Lu, Y.; Chen, W. L.; Wu, Q.; Meng, J. X.; Wang, X. L.; Zhang, Z. M.; Wang, E. B. *Cryst. Growth Des* **2011**, *11*, 458.

(3) (a) Zheng, S. T.; Yuan, D. Q.; Jia, H. P.; Zhang, J.; Yang, G. Y. *Chem. Commun.* **2007**, 1858. (b) Pichon, C.; Mialane, P.; Dolbecq, A.; Marrot, J.; Rivière, E.; Keita, B.; Nadjo, L.; Sécheresse, F. *Inorg. Chem.* **2007**, *46*, 5292. (c) Bareyt, S.; Piligkos, S.; Hasenknopf, B.; Gouzerh, P.; Lacôte, E.; Thorimbert, S.; Malacria, M. *Angew. Chem., Int. Ed.* **2003**, *42*, 3404. (d) Jin, H.; Qi, Y. F.; Wang, E. B.; Li, Y. G.; Wang, X. L.; Qin, C.; Chang, S. *Cryst. Growth Des.* **2006**, *6*, 2693. (e) Hayashi, K.; Murakami, H.; Nomiya, K. *Inorg. Chem.* **2006**, *45*, 8078. (f) Bar-Nahum, I.; Ettedgui, J.; Konstantinovski, L.; Kogan, V.; Neumann, R. *Inorg. Chem.* **2007**, *46*, 5798. (g) Zhang, Z. M.; Li, Y. G.; Wang, Y. H.; Qi, Y. F.; Wang, E. B. *Inorg. Chem.* **2008**, *47*, 7615.

(4) (a) Tan, H. Q.; Li, Y. G.; Chen, W. L.; Liu, D.; Su, Z. M; Lu, Y.; Wang, E. B. *Chem.—Eur. J.* **2009**, *15*, 10940. (b) Yang, H. X.; Guo, S. P.; Tao, J.; Lin, J. X.; Cao, R. *Cryst. Growth Des.* **2009**, *11*, 4735. (c) Jin, H. J.; Zhou, B. B.; Yu, Y.; Zhao, Z. F.; Su, Z. H. *CrystEngComm* **2011**, *13*, 585. (d) Yu, K.; Zhou, B. B.; Yu, Y.; Su, Z. H.; Yang, G. Y. *Inorg. Chem.* **2011**, *50*, 1862. (e) Xu, W. T.; Jiang, F. L.; Zhou, Y. F.; Xiong, K. C.; Chen, L.; Yang, M.; Feng, R.; Hong, M. C. *Dalton Trans.* **2012**, *41*, 7737. (f) Dey, C.; Das, R.; Poddar, P.; Banerjee, R. *Cryst. Growth Des.* **2012**, *12*, 12.

(5) (a) Casan-Pastor, N.; Baker, L. C. W. *J. Am. Chem. Soc.* **1992**, *114*, 10384. (b) Müller, A.; Pope, M. T.; Todea, A. M.; Bögge, H.; Slageren, J. V.; Dressel, M.; Gouzerh, P.; Thouvenot, R.; Tsukerblat, B.; Bell, A. *Angew. Chem., Int. Ed.* **2007**, *46*, 4477.

(6) (a) Baker, L. C. W.; Glick, D. C. *Chem. Rev.* **1998**, *98*, 3. (b) Buckley, R. I.; Clark, R. J. H. *Coord. Chem. Rev.* **1985**, *65*, 167. (c) Mialane, P.; Dolbecq, A.; Lisnard, L.; Mallard, A.; Marrot, J.; Sécheresse, F. *Angew. Chem., Int. Ed.* **2002**, *41*, 2398. (d) López, X.; Fernández, J. A.; Poblet, J. M. *Dalton Trans.* **2006**, 1162.

(7) (a) Barrows, J. N.; Jameson, G. B.; Pope, M. T. *J. Am. Chem. Soc.* **1985**, *107*, 1771. (b) Dablemont, C.; Proust, A.; Thouvenot, R.; Afonso, C.; Fournier, F.; Tabet, J. C. *Dalton Trans.* **2005**, 1831. (c) Zhang, X.; Yi, Z. H.; Zhao, L. Y.; Chen, Q.; Gu, X. M.; Xu, J. Q.; Wang, X. L.; Yang, C.; Xu, X. Z.; Xia, W. J. *Dalton Trans.* **2009**, 9198. (d) Wang, Y.; Xu, L.; Jiang, N.; Zhao, L. L.; Li, F. Y.; Liu, X. Z. *CrystEngComm* **2011**, *13*, 410. (e) Shen, Y.; Peng, J.; Zhang, H. Q.; Chen, C. Y.; Zhang, F.; Bond, A. M. *J. Mater. Chem.* **2011**, *21*, 6995.

(8) (a) Cooper, J. B.; Way, D. M.; Bond, A. M.; Wedda, A. G. *Inorg. Chem.* **1993**, *32*, 2416. (b) Prados, R. A.; Pope, M. T. *Inorg. Chem.* **1976**, *15*, 2547. (c) Way, D. M.; Bond, A. M.; Wedd, A. G. *Inorg. Chem.* **1997**, *36*, 2826. (d) Zhang, J.; Bond, A. M. *Inorg. Chem.* **2004**, *43*, 8263. (e) Fuab, N.; Lu, G. X. *Chem. Commun.* **2009**, 3591.

(9) (a) Müller, A.; Botar, B.; Bögge, H.; Kögerler, P.; Berkle, A. *Chem. Commun.* **2002**, 2944. (b) Tan, S.; Hobday, M.; Gorman, J.; Amieta, G.; Rix, C. *J. Mater. Chem.* **2003**, *13*, 1180. (c) Ritchie, C.; Li, F. Y.; Pradeep, C. K.; Long, D. L.; Xu, L.; Cronin, L. *Dalton Trans.* **2009**, *33*, 6483.

(10) (a) Zhang, X. M.; Wu, H. S.; Zhang, F. Q.; Prikhod'ko, A.; Kuwata, S.; Comba, P. *Chem. Commun.* **2004**, 2046. (b) Yu, K.; Li, Y. G.; Zhou, B. B.; Su, Z. H.; Zhao, Z. F.; Zhang, Y. N. *Eur. J. Inorg. Chem.* **2007**, 5662. (c) Zhang, F. Q.; Zhang, X. M.; Fang, R. Q.; Wu, H. S. *Dalton Trans.* **2010**, *39*, 8256. (d) Yu, K.; Zhou, B. B.; Yu, Y.; Su, Z. H.; Wang, H. Y.; Wang, C. M.; Wang, C. X *Dalton Trans.* **2012**, *41*, 10014.

(11) (a) Leyrie, M.; Hervé, G. *Nouv. J. Chim.* **1978**, *2*, 233. (b) Alizadeh, M. H.; Harmalker, S. P.; Jeannin, Y. *J. Am. Chem. Soc.* **1995**, *107*, 2662. (c) Xue, G.; Vaissermann, J.; Gouzerh, P. *J. Cluster Sci.* **2002**, *13*, 409.

(12) (a) Creaser, I.; Heckel, M. C.; Neitz, R. J.; Pope, M. T. *Inorg. Chem.* **1993**, *32*, 1573. (b) Antonio, M. R.; Soderholm, L. *Inorg. Chem.* **1994**, *33*, 5988. (c) Yoshida, A.; Nakagawa, Y.; Uehara, K.; Hikichi, S.; Mizuno, N. *Angew. Chem., Int. Ed.* **2009**, *48*, 7055.

(13) (a) Sheldrick, G. M. *SHELXL 97, Program for Crystal Structure Refinement*; University of Göttingen: Göttingen, Germany, 1997. (b) Sheldrick, G. M. *SHELXL 97, Program for Crystal Structure Solution*; University of Göttingen: Göttingen, Germany, 1997.

(14) Yu, K.; Zhou, B. B.; Yu, Y.; Su, Z. H.; Wang, C. M.; Wang, C. X . *Inorg. Chem. Commun.* **2011**, *14*, 1846.

(15) (a) Brown, I. D.; Altermatt, D. *Acta Crystallogr., Sect. B: Struct. Sci.* **1985**, *41*, 244. (b) Liu, W.; Thorp, H. H. *Inorg. Chem.* **1993**, *32*, 4102.

(16) (a) Pope, M. T. *Heteropoly and Isopoly Oxometalates*; Springer–Verlag: Berlin, 1983. (b) DasGupta, B.; Katz, C.; Israel, T.; Watson, M.; Zompa, L. *Inorg. Chim. Acta* **1999**, *292*, 172. (c) Patterson, T. A.; Carver, J. C.; Leyden, D. E.; Hercules, D. M. *J. Phys. Chem.* **1976**, *80*, 1700.

(17) (a) Wang, X. L.; Kang, Z. H.; Wang, E. B.; Hu, C. W. *J. Electroanal. Chem.* **2002**, *523*, 142. (b) Wang, X. L.; Kang, Z. H.; Wang, E. B.; Hu, C. W. *Mater. Lett.* **2002**, *56*, 393.

(18) (a) Unoura, K.; Tanaka, N. *Inorg. Chem.* **1983**, *22*, 2963. (b) Fu, H.; Chen, W. L.; Wang, E. B.; Liu, J.; Chang, S. *Inorg. Chem. Acta* **2009**, *362*, 1412.

(19) Martel, D.; Kuhn, A. *Electrochim. Acta* **2000**, *45*, 1829.

(20) Hao, N.; Shen, E. H.; Li, Y. G.; Wang, E. B.; Hu, C. W.; Xu, L. *Eur. J. Inorg. Chem.* **2004**, 4102.

(21) (a) Ley, K. D.; Schanze, K. S. *Coord. Chem. Rev.* **1998**, *171*, 287. (b) Yan, V. W. W.; Lo, K. K. W. *Chem. Soc. Rev.* **1999**, *28*, 323.

(22) Dai, J.-C.; Wu, X.-T.; Fu, Z.-Y.; Cui, C.-P.; Hu, S.-M.; Du, W.-X.; Wu, L.-M.; Zhang, H.-H.; Sun, R.-Q. *Inorg. Chem.* **2002**, *41*, 1391.

(23) Zhang, L. Y.; Liu, G. F.; Zheng, S. L.; Ye, B. H.; Zhang, X. M.; Chen, X. M. *Eur. J. Inorg. Chem.* **2003**, *16*, 2965.

(24) Song, J. L.; Zhao, H. H.; Mao, J. G. *Chem. Mater.* **2004**, *16*, 1884.